Research Article

Reappraisal of the fundamental mechanisms of the sHA14-1 molecule as a Bcl-2/Bcl-XL ligand in the context of anticancer therapy: A cell biological study

Aoula Moustapha[1,2†], Pauline Andreu[2†], François Gonzalvez[2†], Delphine Fradin[2], Jean-Pierre Tissier[3], Phillippe Diolez[4,5], Patrice Xavier Petit[1,2*]

[1]National Center for Scientific Research UMR 8003, Paris City University, SSPIN Neuroscience Institute, Saint-Germain Campus, Paris, Île de France, 75006 France

[2]Department of Genetic and Development, INSERM U567/National Center for Scientific Research UMR 8104, Cochin Institut, Paris, 750014 France

[3]Laboratory of Process Engineering and Food Technologies, INRA Lille Research Center, Villeneuve D'Ascq Cedex, Hauts-de-France, 59591 France

[4]IHU Liryc, Bordeaux University Foundation, Pessac, Bordeaux, Nouvelle-Aquitaine, 33000 France

[5]National Institute of Health and Medical Research, Cardio-Thoracic Research Center, Bordeaux, Nouvelle-Aquitaine, 33000 France

[†]*The authors contributed equally to this work.*

Abstract

Background: HA14-1 is a small-molecule, stable B-cell lymphoma 2 (Bcl-2) antagonist that promotes apoptosis in malignant cells through an incompletely-defined mechanism of action. Bcl-2 and related anti-apoptotic proteins, such as B-cell lymphoma-extra-large [Bcl-XL]), are predominantly localized to the outer mitochondrial membrane, where they regulate cell death pathways. However, the notably short half-life of HA14-1 *in vitro* limits its potential therapeutic application. To address this limitation, a more stable analog, ethyl-2-amino-6-phenyl-4-(2-ethoxy-2-oxoethyl)-4H-chromene-3-carboxylate (sHA14-1), was developed. **Objective:** This study investigated the relationship between sHA14-1 and Bcl-2/Bcl-XL. The sHA14-1 molecule acts as a hormetic substance. Therefore, it is crucial to determine whether the hormetic zone corresponds to a putative therapeutic window, that is, the optimal concentration at which sHA14-1 selectively kills cancer cells overexpressing Bcl-2 or Bcl-XL while causing minimal damage to normal cells. **Methods:** Using classical cell biology and flow cytometry, we examined the main signaling pathways involving Bcl-2 or Bcl-XL, and their modification in the presence of sHA14-1. **Results:** We showed that sHA14-1 exerted a dual effect on mitochondria: (i) it sensitized cells to increased permeability, and (ii) it inhibited adenosine diphosphate-stimulated respiration and uncoupled respiration. At relatively low concentrations, sHA14-1 induced mitochondrial swelling, reminiscent of "pore opening" but with distinct characteristics. Over 30 μM, sHA14-1 caused mitochondrial transition depolarization independent of permeability transition and cell death that resembled secondary necrosis (*i.e.*, occurring after maximal mitochondrial permeability) rather than apoptosis. The balance between apoptotic and necrotic cell death induced by sHA14-1 was also evaluated. **Conclusion:** Our results suggested that sHA14-1 plays a multifunctional role, involving both mitochondria and the endoplasmic reticulum. Its actions are more complex than its originally intended role in targeting anti-apoptotic Bcl-2 family members, which may complicate its potential application as an anticancer therapy.

Keywords: Apoptosis, Bcl-2/Bcl-XL ligand, Bioenergetic, Calcium, Cancer therapy, Mitochondria, PTP pore mitochondria, sHA14-1

***Corresponding author:**
Patrice Xavier Petit (patrice.petit@inserm.fr)

Received: 12 August 2024; Revision received: 26 August 2024; Accepted: 05 November 2024; Published: 30 December 2024

How to cite this article: Moustapha A, Andreu P, Gonzalvez F, *et al.* Reappraisal of the fundamental mechanisms of the sHA14-1 molecule as a Bcl-2/Bcl-XL ligand in the context of anticancer therapy: A cell biological study. *J Biol Methods.* 2024;11(4):e99010040. DOI: 10.14440/jbm.2024.0055

1. INTRODUCTION

Apoptosis, or programmed cell death, is a highly conserved and essential process for development and homeostasis in higher organisms. Defects in the physiological

pathways of apoptosis play a role in a variety of diseases for which effective therapies or preventative measures are not available. For example, insufficient cell death contributes to carcinogenesis, neurodegenerative disorders, and autoimmune diseases. Consequently, a significant interest has arisen in developing therapeutic strategies to modulate key molecules involved in life-or-death decisions in cells [1].

Members of the evolutionarily conserved B-cell lymphoma 2 (Bcl-2) family are important regulators of apoptosis [2-4]. The prototypic members of this family were originally identified at the chromosomal breakpoint of t(14;18)-bearing B-cell lymphomas [5]. Bcl-2-related proteins share at least one of four homologous regions known as Bcl-2 homology (BH) domains (BH1 to BH4). This family includes death antagonists, such as Bcl-2 and B-cell lymphoma-extra-large (Bcl-XL), as well as death agonists, such as Bcl-2 antagonist X (Bax), Bcl-2 homologous antagonist/killer (Bak), and the "BH3-only" subfamily. Bcl-2 family proteins localize to various intracellular organelle membranes, including the mitochondrial outer membrane, the endoplasmic reticulum (ER), and the nuclear membrane [6, 7]. Mitochondrial Bcl-2 and Bcl-XL antagonize the apoptotic signal [4], prevent mitochondrial depolarization, and inhibit the release of apoptosis-inducing factors (*e.g.*, calcium [Ca^{2+}], cytochrome c, and second mitochondria-derived activator of caspase/direct inhibitor of apoptosis-binding protein with low pI). In the ER, Bcl-2 proteins regulate Ca^{2+} homeostasis and prevent cytosolic Ca^{2+} increase through a mechanism that remains poorly understood [8-10]. This mechanism may involve the inositol trisphosphate receptor (IP3R) [10-15], the sarcoendoplasmic reticulum Ca^{2+}-ATPase (SERCA) [8, 16-20], and/or reactive oxygen species (ROS) [19]. Mitochondrial Ca^{2+} uptake, mediated by the IP3R-driven Ca^{2+} release, is locally facilitated by high cytoplasmic Ca^{2+} microdomains near focal contact areas between ER and mitochondria [21], particularly at the level of mitochondria-associated membranes (MAMs) [22]. Ca^{2+} plays a crucial role in linking ER and mitochondrial functions in apoptosis [23]. Both Ca^{2+}-ATPase and SERCA have been implicated in the drug resistance observed in certain cancer therapies [24-28].

High levels of *Bcl-2* gene expression are found in various human cancers [29], including lymphomas and certain solid tumors, such as those in the prostate, breast, lung, and colon. Bcl-2 contributes to neoplastic cell expansion by preventing the normal turnover of cells through physiological apoptosis mechanisms. In addition, Bcl-2 inhibits the cytotoxic effect of many commonly-used anticancer drugs and is implicated in cancer chemoresistance. Indeed, Bcl-2 expression levels in different cancers correlate with resistance to a broad range of chemotherapeutic agents and γ-radiation. Therefore, functional blockade or downregulation of Bcl-2 could restore apoptosis in tumor cells and sensitize them to chemotherapy and radiotherapy. Several approaches have been taken to overcome Bcl-2-mediated chemoresistance, including the use of antisense oligonucleotide injections to reduce Bcl-2 expression [30] and the development of small molecules to inhibit Bcl-2 activity [31,32].

Despite its critical role in apoptosis, the mechanisms governing Bcl-2 regulation are not fully understood. It is known that Bcl-2 family members form hetero- or homotypic dimers, and these protein-protein interactions are essential for their biological functions. The three-dimensional structures of Bcl-XL (which is highly homologous to Bcl-2) [33] and the Bcl-XL/Bak complex [34], resolved by X-ray crystallography and nuclear magnetic resonance, revealed an elongated hydrophobic cleft formed by the BH1, BH2, and BH3 domains. Mutational analyses have shown that this cleft constitutes the binding site for other Bcl-2 family members and is required for the anti-apoptotic function of Bcl-2. Thus, blocking this binding pocket could prevent Bcl-2 dimerization, thereby inhibiting its anti-apoptotic action and releasing Bax/Bak, which subsequently execute the cell death program. Various strategies have been employed to create inhibitors targeting this pocket, including synthetic peptides [35,36], organic molecules [36-38], and physiological compounds such as antimycin A [39] and tetrocarcin A [40,41]. In recent years, small-molecule Bcl-2 antagonists have been developed, some of which have been tested in clinical trials for treating hematopoietic malignancies and solid tumors [42-45].

The first BH3 mimetic designed was HA14-1 [36,46], although it suffered from poor specificity and ROS-associated toxicity. HA14-1 was discovered through computer screening as a ligand for the hydrophobic pocket of Bcl-2 and was the first molecule shown [36,46] to exhibit "selective cytotoxicity" against drug-resistant cancer cells that overexpress anti-apoptotic Bcl-2 family members. Subsequently, a more stable and ROS-free Bcl-2 antagonist, ethyl-2-amino-6-phenyl-4-(2-ethoxy-2-oxoethyl)-4H-chromene-3-carboxylate (sHA14-1), was developed. This compound bypasses drug resistance mechanisms and has shown synergy with cancer therapies in human leukemic cells [44]. Moreover, sHA14-1 has been reported to enhance the efficacy of other cancer therapies [47,48]. Given that many therapeutic molecules exhibit hormetic properties, it is critical to precisely determine the dose that optimizes therapeutic efficacy. More recently, other BH3 mimetics, such as ABT-737, ABT-263, and ABT199, have been developed with greater specificity for Bcl-2 and/or Bcl-XL (and sometimes myeloid cell leukemia-1 [Mcl-1]). The canonical action of Bcl-2 family proteins involves binding the hydrophobic pocket of anti-apoptotic proteins (Bcl-2, Mcl-1, Bcl-XL, A1 [also known as Bfl-1 in humans], and Bcl-w) through

their BH3 domain. This interaction induces the release and, consequently, the activation of the pro-apoptotic proteins Bax and Bak, which oligomerize to disrupt the mitochondrial outer membrane [5-11]. The release of cytochrome c and other apoptogenic factors into the cytoplasm promotes apoptosome formation, involving the association of its two primary components, that is, cytochrome c and the cytosolic apoptotic protease activating factor-1, along with deoxyadenosine triphosphate. This event, in turn, activates caspase 9/3, initiating a cascade of effector caspases that cleave hundreds of proteins, thereby dismantling the cell in an orderly manner.

However, it remains unclear whether the toxicity exhibited by sHA14-1 in cells with low expression of Bcl-2 and Bcl-XL is sufficiently low to allow for its use in cancer therapy. sHA14-1 is cell-permeable and has been proposed to induce cell death by inhibiting Bcl-2. Thus, it represents a promising candidate for the development of a new chemotherapeutic agent. Nevertheless, its exact mechanism of action in the cell death pathway is not yet fully understood. In this study, we used sHA14-1, which has been demonstrated to be more stable than HA14-1 and ROS-free. It has been shown that sHA14-1 can bind to all three BH domains (BH1, BH2, and BH3) of Bcl-2, while interacting with only the BH1 and BH3 domains of Bcl-XL to inhibit its functionality by binding to critical amino acids of the protein [48].

To be an effective cancer treatment, sHA14-1 must specifically target tumor cells, meaning its activity should be limited to inhibiting Bcl-2 (and/or Bcl-XL) and should induce cell death exclusively through apoptosis. Due to its enhanced stability, we used sHA14-1 as an analog. In this study, we found that this small molecule targets both the mitochondria and the ER in cells expressing Bcl-2 and/or Bcl-XL. The objective of the present study was to identify and describe the molecular mechanisms underlying apoptosis induction and the occurrence of secondary-necrosis (cell death following strong apoptotic induction) caused by sHA14-1. We also aimed to determine whether there are any differences between Bcl-2 and Bcl-XL in cells treated with sHA14-1.

2. MATERIALS AND METHODS

2.1. Animals

Three types of mice were used in this study: control mice (C57/Bl6) and age- and sex-matched congenic mice expressing either a *Bcl-2* transgene [49] or a *Bcl-XL* transgene [21,51], both controlled by the L-type pyruvate kinase gene promoter.

2.2. Cells and compounds

In this study, we used sHA14-1 [44], the synthesis of which was recently described [47] and which is more stable than HA14-1 [49] (kindly provided by Dr. C. Xing, University of Minnesota, Minneapolis). Due to its poor solubility in PBS, sHA14-1 was first dissolved in pure dimethyl sulfoxide (DMSO) and then diluted with ultrapure water to the desired concentrations, ensuring that the final DMSO concentration was less than 0.5%. Freshly prepared solutions of sHA14-1 were used for all experiments.

Wild-type human Henrietta Lacks (HeLa) cells were obtained from the American Type Culture Collection (ATCC, United States) and cultured in RPMI-1640 with GlutaMax-1, 10% heat-inactivated fetal calf serum, and 100 U/mL penicillin/streptomycin at 37°C under 5% CO_2. HeLa cells transfected with the human *BCL-2* gene (HeLa-BCL-2/HBcl-2, kindly provided by Dr. N. Israel, Pasteur Institute, France) [51] or with the human *BCL-XL* gene (HeLa-BCL-XL/H-Bcl-XL, kindly provided by Dr. K. Schulze-Osthoff [52], University of Muenster, Germany), as well as control cells transfected with the pcDNA3.1 vector containing the neomycin-resistance gene (HeLa-Neo/HNeo), were cultured under the same conditions and, when necessary, selected in the same medium containing 500 mg/mL G-418.

2.3. Cytofluorimetric determination of apoptosis-associated alterations

Flow cytometrical analysis was performed on a FACSCalibur flow cytometer (Becton Dickinson, United States) using the CellQuest software for acquisition and analysis. The light-scatter and forward-scatter channels were set to linear gains, while the fluorescence channels were set to a logarithmic scale. A total of 10,000 cells were analyzed for each condition. Cell size and density were assessed using forward and side-angle scatters to exclude debris and aggregates. To determine changes in mitochondrial membrane potential ($\Delta\Psi m$), 1×10^6 cells were incubated with 3,3'-dihexyloxacarbocyanineiodide [$DiOC_6(3)$, 40 nM] at room temperature (RT) for 15 minutes, and gated for parametric histograms on FL1. Chloromethyl X-rosamine (CMXRos, 100 nM) was also used for mitochondrial $\Delta\Psi m$ measurement (FACSCalibur FL2 channel). Exposed phosphatidylserines on the outer plasma membrane were measured by staining cells with 1 mg/mL annexin V-fluorescein isothiocyanate (FITC) (Beckman Coulter Immunotech, France) for 10 minutes at 4ºC, followed by the addition of propidium iodide (PI, 1 mg/mL). To distinguish necrosis from apoptosis, cell viability was determined by staining with PI (1 mg/mL) and gating the cells to obtain biparametric histograms (FL1 [BP 525 ± 20 nm] versus FL3 [LP 630 nm]). A second assessment of apoptotic and necrotic cells was performed by employing the Membrane Permeability/Dead Cell Apoptosis Kit with YO-PRO®-1 and PI for Flow Cytometry (Molecular Probes, n° V13243, Thermo Fisher Scientific, USA). YO-PRO-1 dye and PI solutions (1 mg/mL) were added (2.0 µL each)

to 1.0 mL aliquots of suspended cells, which were incubated for at least 20 minutes at RT. The samples were then flow cytometrically analyzed and gated to obtain biparametric histograms (FL1 [BP 525 ± 20 nm] versus FL3 [LP 630 nm]). The three populations were analyzed as follows: normal cells (YOPRO-1$^-$/PI$^-$), apoptotic cells (YOPRO-1$^+$/PI$^-$ or slightly PI-positive), and necrotic-like cells (YOPRO-1$^+$/PI$^+$), the latter representing cells undergoing secondary necrosis to apoptosis, as per Thermo Fisher instructions.

Caspase-3 activity was monitored using a detection kit (Phiphilux, G_1D_2 - 090109, Calbiochem, OncoImmunin's Reagents, USA) according to the manufacturer's instructions. Briefly, cells were harvested and incubated for 30 minutes at 37°C in the presence of a cell-permeant substrate, Red-DEVD-fmk. Cells were washed twice and analyzed by flow cytometry. Bok-Asp(Ome)-FMK (Bok-D 500 nM, Abcam ab142036) was used as a pan-caspase inhibitor (more efficient and less susceptible to toxic side effects than the caspase inhibitor Z-VAD-fmk). Cells were also selected based on viability, as assessed by double staining with TO-PRO-3 (2 mg/mL). Calcium green (stock solution at 1 mM, used at 2 µM) and dichlorofluorescein diacetate (DCFH-DA, stock solution at 1 mM, used at 2 µM) were used for Ca^{2+} flux and ROS measurements, respectively. Ethylene glycol-bis(β-aminoethyl ether)-N,N,N',N'-tetraacetic acid (EGTA) was added to cell cultures at 1 mM. Mitochondria-targeted antioxidant Mito-Q_{10} (500 nM), a coenzyme Q analog attached to a triphenylphosphonium cation to direct the antioxidant to the mitochondrial matrix, was used. In addition, 6-hydroxy-2,5,7,8-tetramethylchroman-2-carboxylic acid (Trolox, 1 µM), a soluble, membrane-permeable antioxidant, and manganese (III) tetrakis (4-benzoic acid) porphyrin chloride (MnTBAP, 5 µM), an MnSOD mimetic, were used as antioxidants.

2.4. Scanning electron microscopy

Cell suspensions were fixed for at least 4 hours in a 1.25% (volume/volume) glutaraldehyde solution in 0.1 M sodium cacodylate buffer (pH 7). Aliquots containing approximately 1×10^6 cells, or fewer cell aggregates, were filtered through a 25 nm diameter, 0.2 nm porosity Anodisc (Whatman, 1001325, United Kingdom). The filters were then rinsed five times in sodium cacodylate buffer, and subsequently rinsed five times in ultrapure water. The samples were dehydrated in a graded ethanol series (50%, 70%, 95%, and twice in 100%). After dehydration, the filters were soaked in isopentyl acetate before being subjected to critical point drying in CO_2 using an EMSDCOPE CPD 750 apparatus (Elexience, France). The filters were then attached to large scanning electron microscopy stubs using double-sided tape and coated with gold-palladium by cathodic spreading in a Polaron E 5100 coater (JEOL Ltd, Japan). A JEOL JSM35CF (JEOL Ltd, Japan) or an S-3000 Hitachi scanning electron microscope (Hitachi Ltd, Japan), operating at 15 kV voltage, was used to observe the samples and capture photomicrographs.

2.5. Purification of mouse liver mitochondria, and measurement of respiratory activity, and membrane potential

Three- to six-week-old C57/Bl6 mice were euthanized by cervical dislocation. Mitochondria were isolated from liver tissue in medium H (pH 7.2), which contained 0.3 M sucrose, 5 mM N-tris[Hydroxymethyl]-methyl-2-aminoethanesulfonic acid (TES), 0.2 mM EGTA, and 0.1% bovine serum albumin (BSA; weight/volume; pH 7.2 [53] To separate intact mitochondria from broken ones, the organelles were layered on a Percoll gradient (10 minutes at 8500 × g), consisting of three layers: 18%, 30%, and 70% (weight/volume) Percoll in medium H. Mitochondria were collected from the 30%/70% interface and washed with medium H. The same procedure was used to prepare mitochondria from Bcl-2 [49] and Bcl-XL [50] transgenic mice.

Percoll-purified mitochondria were resuspended in a respiratory medium (R), which consisted of 40 mM sucrose, 100 mM potassium chloride, 5 mM magnesium chloride, 10 mM TES, 10 mM monopotassium phosphate (pH 7.2), 1 mM ethylene glycol diacetate, and 0.1% BSA. For respiratory measurements, the mitochondrial protein concentration was adjusted to 0.33 mg/mL in a final volume of 1.5 mL of medium R maintained at 25ºC. Oxygen uptake and $\Delta\Psi m$ were simultaneously monitored in an oxygen-electrode chamber (Oxygraph, Hansatech Instruments Ltd., United Kingdom), using a Clark-type electrode to measure oxygen uptake and a tetraphenylphosphonium cation (TPP^+)-sensitive electrode to determine $\Delta\Psi m$. Mitochondrial $\Delta\Psi m$ was calculated according to Kamo *et al.* [54], with TPP^+ binding corrected based on the method described by Rottenberg [55].

2.6. Mitochondrial swelling

Mitochondrial swelling was estimated by the decrease in absorbance at 520 nm on a Uvikon 930 spectrophotometer (Kontron Instruments, France). The medium contained 250 mM sucrose, 20 mM Tris-3-(N-morpholino) propanesulfonic acid (pH 7.2), 2 µM rotenone, 10 µM EGTA, and 300 µM inorganic phosphate (P_i) -Tris. The addition of P_i ensured optimal succinate transport activity and subsequent succinate dehydrogenase activity. The presence of EGTA at low concentration (10 µM) improved experimental reproducibility. Cyclosporin A (CsA) was used at 2 µM, and Ca^{2+} was added at 25 mM.

2.7. Statistical analysis

Statistical analyses were carried out using the Kruskal–Wallis test (*p<0.05; **p<0.01; and ***p<0.001). Data are expressed as mean± standard deviation (SD), with the number of experiments cited as n.

3. RESULTS

3.1. sHA14-1 induces apoptosis and/or necrosis in Henrietta Lacks cells

sHA14-1 was designed to occupy the surface pocket of Bcl-2 or Bcl-XL, which is critical for their anti-apoptotic functions [49]. This raises the possibility that sHA14-1 may antagonize Bcl-2 and Bcl-XL function, triggering apoptosis through the release of pro-apoptotic molecules such as Bax or Bak. However, in a previous study [49], none of the experiments were designed to evaluate the effect of HA14-1 on wild-type cells that have little or no Bcl-2 protein, which could help determine if the drugs interact with the mitochondrial outer membrane. Given that the original HA14-1 molecule has a short half-life *in vivo*, we used the more stable compound, sHA14-1, in our experiments on cell death [44]. HNeo cells (empty vector), HBcl-2, and HBcl-XL (Figure 1) were treated for 4 h with increasing concentrations of sHA14-1 (from 0 to 100 μM). Surprisingly, sHA14-1 induced death in all three cell types in a concentration-dependent manner (Figure 1D-F). At low concentrations of sHA14-1 (≤50 μM, with an IC50 value of 42 μM), Bcl-2 appeared to exert its anti-apoptotic effect (Figure 1E). Similarly, the protective effect of Bcl-XL was evident at lower sHA14-1 concentrations (IC50=42 μM) (Figure 1F). We also observed that the death mechanisms involved in the control HNeo cells were primarily apoptotic at low concentrations of sHA14-1 (with a low IC50 value of 18 μM), followed by late-stage necrosis. In contrast, in HBcl-2 and HBcl-XL cells, cell death was initiated at much higher concentrations (42 μM for HBcl-2 and 38 μM for HBcl-XL). These deaths seemed to be primarily necrotic, or possibly the result of a very rapid apoptotic process involving "unspecific permeabilization" of the outer membrane, which prevented the apoptotic phases from being fully detected (Figure 1E and F).

Apoptosis can be differentiated from secondary necrosis using a double-staining technique that takes advantage of the differential penetration of two fluorescent probes: YO-PRO-1 and PI. This technique allowed us to determine the ratio of apoptotic cells (YO-PRO-1$^+$PI-) to necrotic cells (YO-PRO-1$^+$PI$^+$) for all treatments. HNeo cells underwent typical apoptosis at low sHA14-1 concentrations (0–40 μM), while they became necrotic at higher concentrations (Figure 1D). In contrast, HBcl-2 cells were protected by Bcl-2 at low sHA14-1 concentrations (up to 40 μM) (Figure 1E), whereas protection against death by Bcl-XL in HBcl-XL cells was effective only at sHA14-1 concentrations up to 30 μM (Figure 1F). Notably, HBcl-2 and HBcl-XL cells were more likely to undergo secondary necrosis at higher concentrations of sHA14-1 than HNeo cells (Figure 1F).

3.2. sHA14-1 induces apoptosis and/or necrosis through the mitochondrial pathway and caspase activation

To examine the mechanisms of cell death induced by sHA14-1, we investigated whether a sHA14-1 treatment was accompanied by changes in ΔΨm and caspase-3 activation in the three cell types (Figure 2). We observed a clear correlation between caspase-3 activation and a decrease in ΔΨm for all three cell types. As previously noted with late markers of apoptosis (annexin V-FITC/propidium iodide [PI] staining or YO-PRO-1/PI double staining), HBcl-2 and HBCL-XL cells were protected against early apoptotic events (*i.e.*, mitochondrial changes and caspase-3 activation were low) at low sHA14-1 concentrations (<20 μM). However, both cell types displayed a marked acceleration of both events at higher concentrations. Caspase activation, but not the drop in ΔΨm, was sensitive to the caspase inhibitor Bok-D (Figure 2).

3.3. Cyclosporin A partially inhibits sHA14-1-induced cell death

The externalization of phosphatidylserine residues on the outer surface of cells is a hallmark of apoptosis. Treatment with CsA, a permeability transition pore (PTP) inhibitor, reduced annexin-V staining of phosphatidylserine residues on the plasma membrane of HNeo cells exposed to 30 μM sHA14-1, indicating that CsA may reduce apoptosis in these cells (Figure 3A). We then examined the effect of CsA on the generation of apoptotic (Figure 3B) or secondary necrotic (Figure 3C) HNeo cells in the presence of sHA14-1. This analysis confirmed a partial, concentration-dependent protective effect of CsA. Another PTP inhibitor, bongkrekic acid, also protected cells from sHA14-1-induced cell death (data not shown). CsA treatment inhibited apoptosis by approximately 50% (Figure 3B), whereas necrosis was less affected (Figure 3C). Nevertheless, these results suggest that sHA14-1 may increase PTP-mediated mitochondrial permeability, and that this effect could partially contribute to its mechanism of inducing cell death. The remaining 50% of cell death may result from the interaction of sHA14-1 with the ER (where Bcl-2 and Bcl-XL may be present) and/or from direct interaction with other organelle membranes.

3.4. Scanning electron microscopy

All HeLa cells exhibited a round morphology, with HBcl-XL cells being slightly larger than the HNeo or the HBcl-2 cells (Figure 4). HNeo cells treated with sHA14-1 at 30 μM showed typical apoptotic bodies (Ap), along with

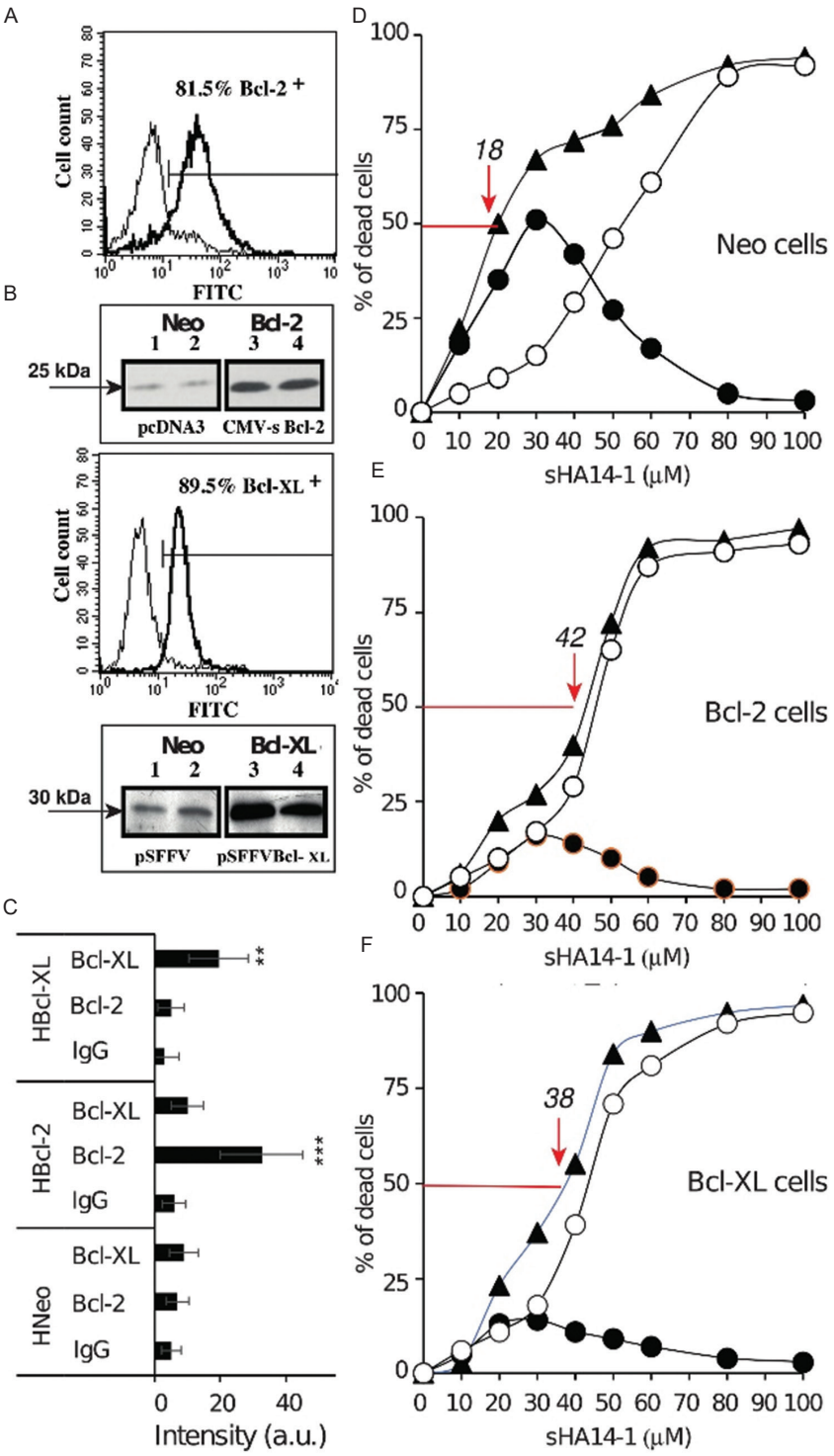

Figure 1. Cell death induction by sHA14-1. (A and B) Flow cytometric analysis and Western blotting of Bcl-2 (molecular weight [MW] 25 kDa) and Bcl-XL (MW 30 kDa) expression in HeLa cells. The percentage of Bcl-2- and Bcl-XL-positive cells is shown relative to the control Neo cells. (C) Histogram showing the presence of Bcl-2 and Bcl-XL in HeLa cells. Flow cytometrical data are based on six independent experiments, expressed as mean ± SD. Statistical significance was assessed using one-way ANOVA with the least significant difference *post hoc* multiple (**p*<0.05, ***p*<0.01, and ***p<0.001). (D-F) Determination of the IC50 for sHA14-1, total cell death induced by various concentrations of sHA14-1 (black triangles), along with the proportions of apoptotic (black circles) and necrotic (hollow circles) cells for HNeo (D), HBcl-2 (E), and HBcl-XL (F). Apoptotic and necrotic cells were identified by YO-PRO-1/PI staining, based on differences in plasma membrane permeability. Apoptotic cells (black circles) are YOPRO-1+/PI-, while necrotic cells (hollow circles) are YOPRO-1+/PI+. The black triangle curve represents the sum of apoptotic and necrotic cells, indicating total cell death, excluding debris and aggregated cells.

Abbreviations: Bcl-XL: B-cell lymphoma-extra-large; Bcl-2: B-cell lymphoma 2; CMV: Cytomegalovirus; FITC: Fluorescein isothiocyanate; IgG: Immunoglobulin G; pSFFV: Posterior short-segment fixation including the fractured vertebra.

Notes: HNeo represents control Henrietta Lacks (HeLa) cells transfected with the pcDNA3.1 vector containing the neomycin-resistance gene. HBcl-2 refers to HeLa cells transfected with the human *BCL-2* gene. HBcl-XL are cells transfected with the human *BCL-XL* gene.

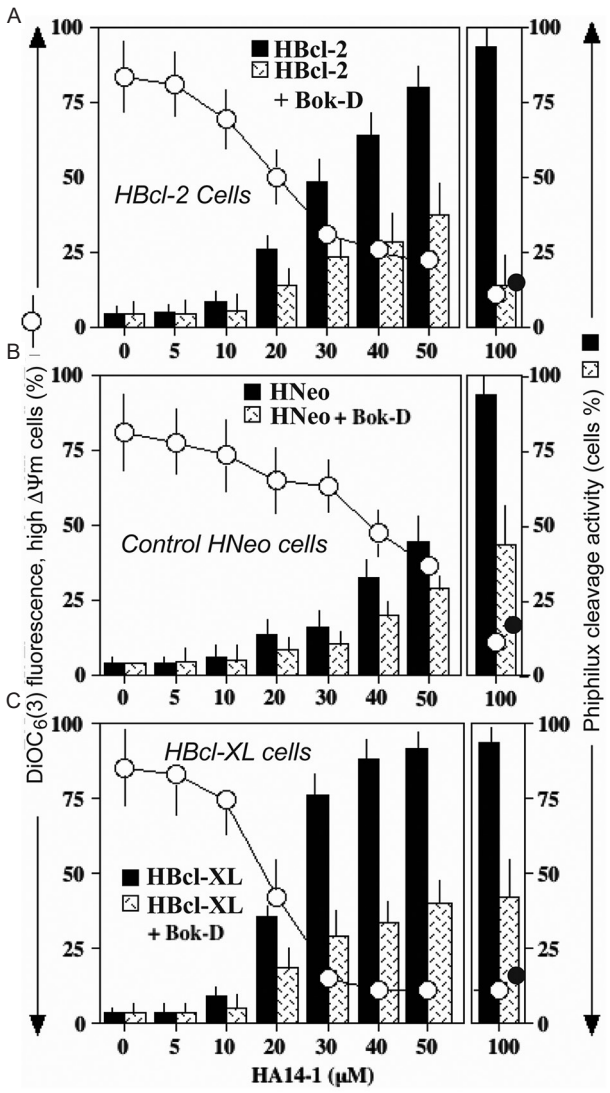

Figure 2. Cell death signal transduction induced by various concentrations of sHA14-1. Membrane potential (ΔΨm) and caspase-3 activity were measured using 3,3'-dihexyloxacarbocyanineiodide ($DiOC_6(3)$) staining and DEVD cleavage activity (Phiphilux), respectively. Bok-D-OMe-FMK (Bok-D was used at 100 nM as pan-caspase inhibitor, Abcam ad 142036). The effect of Bok-D is denoted by • for the higher sHA14-1 concentration, since Bok-D has no effect on mitochondrial ΔΨm. The curve for $DiOC_6(3)$ staining in the presence of Bok-D is not shown, as its inclusion would make the figure too cluttered and difficult to read.

Abbreviations: Bcl-XL: B-cell lymphoma-extra-large; Bcl-2: B-cell lymphoma 2.

Notes: HNeo represents control Henrietta Lacks (HeLa) cells transfected with the pcDNA3.1 vector containing the neomycin-resistance gene. HBcl-2 refers to HeLa cells transfected with the human *BCL-2* gene. HBcl-XL are cells transfected with the human *BCL-XL* gene.

a few cells that remained unchanged in size but were quite rugose, presumably due to the presence of numerous holes in their plasma membrane (Ap+, secondary necrosis, Sn). The HBcl-2 and HBcl-XL cell preparations exhibited a greater number of cells with this irregular morphology, indicating a higher proportion of necrotic-like cells (*i.e.*, cells undergoing necrosis shortly after the apoptotic process).

3.5. sHA14-1 disrupts mitochondrial bioenergetics

Given that CsA influenced sHA14-1-mediated cell death (Figure 3), we next investigated whether sHA14-1 affects mitochondrial respiration and ΔΨm in isolated mitochondria from wild-type mice and mice overexpressing Bcl-2 or Bcl-XL (Figure 5).

For this purpose, we used mitochondria purified from the livers of wild-type mice and Bcl-2-overexpressing mice. We found that sHA14-1 significantly affected both mitochondrial respiration and ΔΨm in Bcl-2-overexpressing mitochondria (Figure 5A-C). The Percoll-purified mitochondria from Bcl-2-overexpressing mice were well-coupled, with a respiratory control ratio greater than 5.16 (Figure 5A-C and Table 1). On the first adenosine diphosphate (ADP)/adenosine triphosphate transition, which allowed for the controlled transition between the phosphorylated state (state 3) and non-phosphorylated (state 4) states, sHA14-1 was added, resulting in an immediate inhibition of state 3 respiration and ΔΨm, while state 4 respiration increased. Specifically, respiration decreased from 5.16 to 3.9, and ΔΨm slightly decreased from 182 to 161 mV (Figure 5B and Table 1). A higher sHA14-1 concentration (50 nM) yielded similar results, whereas a 100 nM concentration caused a substantial drop in ΔΨm (to 116 mV, near the resting potential). Both state 3 (ADP-stimulated phosphorylation) and state 4 (non-phosphorylation) oxidation rates followed the same pattern, with a decrease in state 3 respiration and an increase in state 4 respiration, indicative of mitochondrial uncoupling (Figure 5C and Table 1). Thus, sHA14-1 induces a typical uncoupling effect on mitochondrial respiration (Figure 5D). Our results also suggest that Bcl-2 and Bcl-XL effectively mitigate the effects of sHA14-1 at low concentrations (25 nM), probably due to the interaction of sHA14-1 with their surface pockets. At higher concentrations (up to 100 nM), these pockets may become saturated, allowing sHA14-1 to exert its toxic side effects directly on the mitochondrial membranes (Figure 5C and Table 1).

Regarding the bioenergetic consequences of the sHA14-1 treatment at a low dose (25 nM), mitochondria from Bcl-2 and Bcl-XL-overexpressing cells exhibited resistance to uncoupling and significant decrease in ΔΨm, compared to HNeo mitochondria, which were sensitive due to the lack of anti-apoptotic proteins that could sequester some of the sHA14-1 molecules (Table 1). At concentrations above 25 nM, all mitochondrial types became highly sensitive to sHA14-1, showing a marked decrease in ΔΨm drop and uncoupling. State 3 respiration (ADP-stimulated) was inhibited, while state 4 respiration increased, indicating uncoupling from ADP-stimulated respiration and a marked decrease in respiratory control (Table 1).

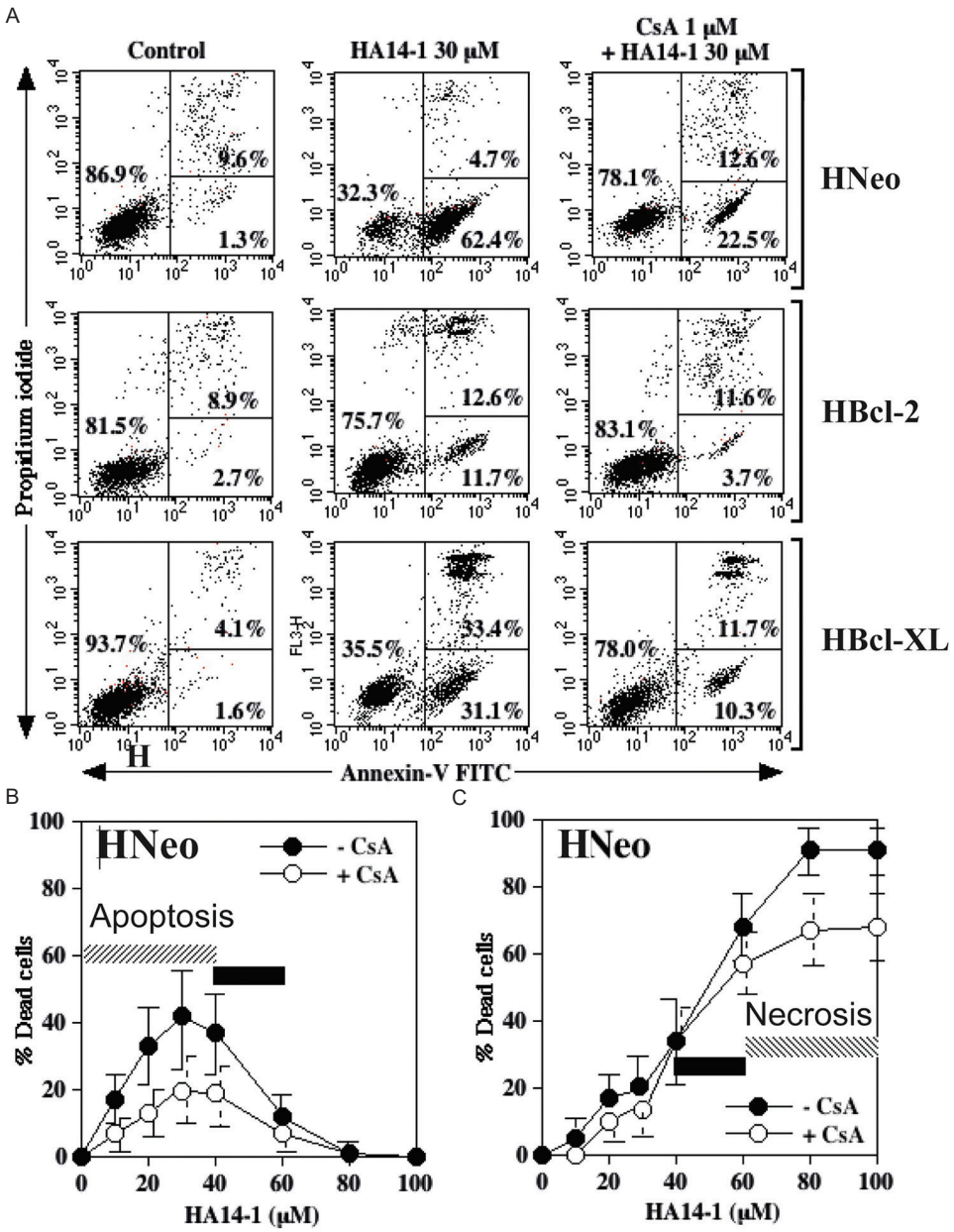

Figure 3. sHA14-1 induction of apoptosis and mitochondrial membrane permeability transition. (A) Apoptosis and necrosis in response to sHA14-1 treatment were assessed using annexin-V-fluorescein isothiocyanate (FITC) staining. Cyclosporin A (CsA; 1 mM) was used as an inhibitor of the PTP pore opening in each Henrietta Lacks (HeLa) cell line. (B and C) Responses to sHA14-1 obtained as a function of its concentration, and in the presence of the permeability transition pore inhibitor, CsA (1 mM). In (b), cells that are annexin V-FITC-positive and propidium iodide (PI))-negative are considered characteristic apoptotic cells. In (c), cells that are annexin V-FITC-positive and PI-positive are classified as necrotic (or necrotic-like cells following apoptosis).

Abbreviations: Bcl-XL: B-cell lymphoma-extra-large; Bcl-2: B-cell lymphoma 2.

Notes: HNeo represents control HeLa cells transfected with the pcDNA3.1 vector containing the neomycin-resistance gene. HBcl-2 refers to HeLa cells transfected with the human *BCL-2* gene. HBcl-XL are cells transfected with the human *BCL-XL* gene.

3.6. sHA14-1 induces an unusual swelling of isolated mitochondria

In the presence of PTP openers, such as tert-butyl hydroperoxide (tBHP), curcumin, and Ca^{2+}, we observed that isolated mitochondria swelled to an unusually large size, consistent with PTP opening (Figure 6). In the case of Ca^{2+}, a typical three-phase process was observed. Initially, Ca^{2+} entered the mitochondria, causing slight mitochondrial shrinkage (condensation) with an increase in absorbance. This event was followed by a full PTP opening, leading to a decrease in absorbance in a characteristic "S" curve, reaching a maximum when the PTP was widely open (Figure 6A). For both curcumin (20 mM) and tBHP (5 mM), the condensation

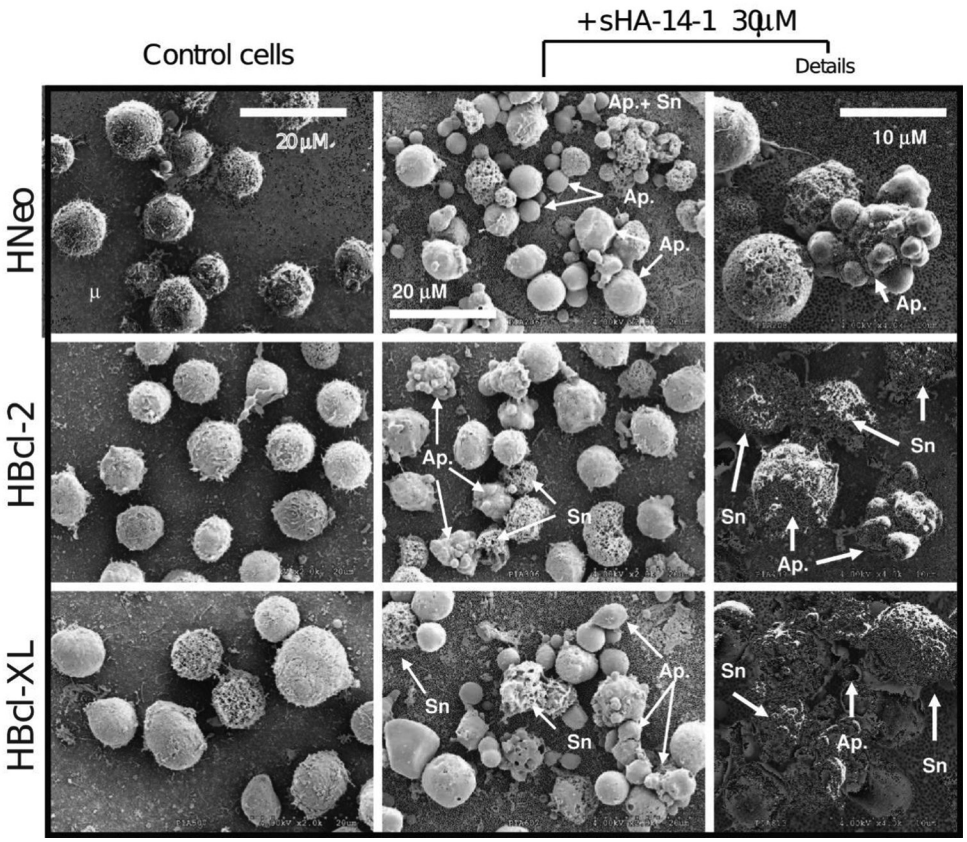

Figure 4. Scanning electron microscopy of Henrietta Lacks cells. The three Henrietta Lacks (HeLa) cell lines (HNeo, HBcl-2, and HBCL-XL) were exposed to 30 µM sHA14-1 and visualized using scanning electron microscopy. The scale is 20 µm for the left and central images and 10 µm (×2) for the enhanced images. Secondary necrosis is characterized by cells of normal size that exhibit a high degree of rugosity, due to the presence of small holes in their plasma membrane. Necrotic cells were highly permeable to propidium iodide (PI), as analyzed by flow cytometry, and showed a higher degree of side scatter than apoptotic cells.
Abbreviations: Ap: Apoptotic bodies; Sn: Secondary necrosis; Bcl-XL: B-cell lymphoma-extra-large; Bcl-2: B-cell lymphoma 2.
Notes: HNeo represents control HeLa cells transfected with the pcDNA3.1 vector containing the neomycin-resistance gene. HBcl-2 refers to HeLa cells transfected with the human *BCL-2* gene. HBcl-XL are cells transfected with the human *BCL-XL* gene.

Table 1. Titration of the effects of sHA14-1 on mitochondrial membrane potential and respiratory rates during state 3 or state 4 respiration in mitochondria isolated from HNeo, HBcl-2, and HBcl-XL cells treated with 25 or 50 nM sHA14-1. The respiratory control are given

Type of cell and concentration of sHA14-1	ΔΨm loss		Uncoupling	Inhibition	Decrease
	ΔΨm4	ΔΨm3	$V_{ox}4$	$V_{ox}3$	RC
Neo cell mitochondria	178±5	128±7	42±4	215±11	5.11
sHA14-1 25 nM	157±5	108±5	66±5	193±10	2.92
Bcl-2 cell mitochondria	182±11	139±6	43±4	222±10	5.16
sHA14-1 25 nM	161±5	129±4	53±5	180±8	3.39
sHA14-1 50 nM	146±4	128±5	66±7	154±7	2.33
Bcl-XL cell mitochondria	179±12	135±7	39±4	212±10	5.43
sHA14-1 25 nM	159±5	127±4	54±5	176±8	3.25
sHA14-1 50 nM	145±8	123±9	59±9	124±8	2.10

Notes: ΔΨm indicates mitochondrial membrane potential, expressed in millivolts (mV), while V_{ox} represents respiratory rate, presented as nmol O_2/min/mg protein. RC refers to the respiratory control ratio. HNeo represents control Henrietta Lacks (HeLa) cells transfected with the pcDNA3.1 vector containing the neomycin-resistance gene. HBcl-2 refers to HeLa cells transfected with the human *BCL-2* gene. HBcl-XL are cells transfected with the human *BCL-XL* gene.
Abbreviations: Bcl-2: B-cell lymphoma 2; Bcl-XL: B cell lymphoma-extra-large.

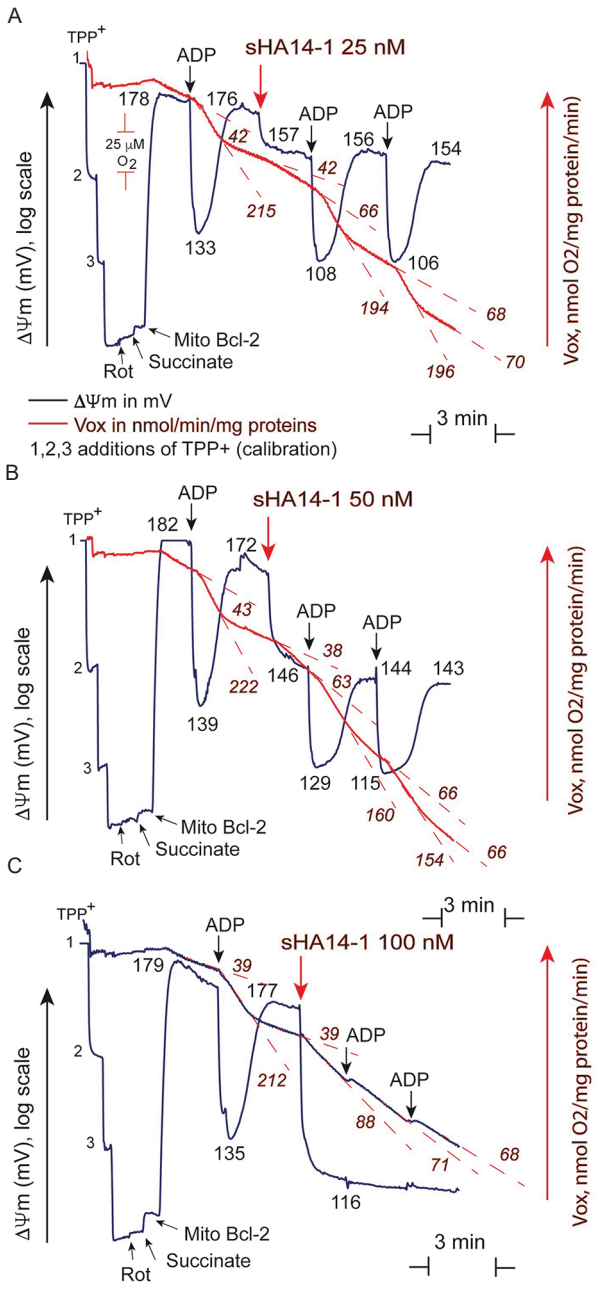

Figure 5. Bioenergetics of purified isolated mitochondria incubated with sHA14-1. (A and B) Recordings of membrane potential (ΔΨm, measured by tetraphenylphosphonium cation [TPP+] electrode) and oxygen consumption (measured by Clark electrode) of Percoll-purified mitochondria. The data shown were obtained for Bcl-2 expressing mitochondria. The numbers in red along the trace represent respiratory rate (V_{ox}) in nmol O_2/mg protein/min, whereas the numbers in blue indicate the ΔΨm in mV. Black arrows indicate the points at which TPP+ was used to calibrate the electrode. Measurements were performed in the presence of succinate (1 mM) and rotenone (1 µM).

Abbreviations: ADP: Adenosine diphosphate; Bcl-2: B-cell lymphoma 2; Mito: Mitochondria; Rot: Rotenone.

phase was absent, and the PTP opening also followed an "S" curve (Figure 6A). Similarly, sHA14-1 treatment did not induce an "S" curve, and the swelling observed was moderate, even at 50 nM (red curve in Figure 6A).

In Bcl-2-overexpressing mitochondria, the swelling was barely evident, only occurring at 100 nM sHA14-1 (Figure 6B), and in all cases, CsA inhibited the residual swelling. In the classic Ca^{2+}-inducible PTP opening mechanism, mitochondria first condense as Ca^{2+} enters the matrix, followed by swelling as the PTPs open (Figure 6A). Incubation with CsA maintained the mitochondria in a condensed form. However, this pattern was not observed with sHA14-1 treatment. Interestingly, the swelling in these mitochondria appeared to be associated with PTP opening (Figure 6A-C), as if sHA14-1 molecules structurally affected the pore itself. This could reflect a non-specific interaction of sHA14-1 with mitochondrial membranes, potentially indicating a toxic-like effect. The histogram in Figure 6C summarizes the data, showing that sHA14-1 might have a pore-like effect on mitochondria, which is modulated by the presence of Bcl-2 or Bcl-XL at the mitochondrial membrane surface.

3.7. sHA14-1 induces endoplasmic reticulum calcium release and mitochondrial reactive oxygen species production

Mitochondria are key physiological targets and platforms for intracellular Ca^{2+} signaling, particularly in the context of apoptotic cell death [23,51]. Mitochondrial Ca^{2+} uptake is locally facilitated by high cytoplasmic calcium Ca^{2+} microdomains, which arise from IP3R-mediated Ca^{2+} release at focal contact areas between the ER and mitochondria, known as MAMs [21]. Mitochondria are structurally and functionally diverse, and certain subsets are capable of interacting with other organelles [53,54]. The localized Ca^{2+} concentration that regulates the interaction between IP3Rs and mitochondria is particularly important at stable contact sites between the ER and mitochondria [53-57]. These connections are required to propagate the ER signals to mitochondria. Tightened connections, whether synthetic or naturally occurring during apoptosis, make mitochondria more susceptible to Ca^{2+} overload and subsequent PTP opening. To understand whether Ca^{2+} is directly involved in the action of sHA14-1, we used CG and flow cytometry to monitor intracellular Ca^{2+} levels in a time-dependent manner. The addition of low concentrations of sHA14-1 (5 µM) to HNeo cells resulted in an immediate increase in Ca^{2+} (Figure 7A and D), which was more pronounced at higher concentrations of sHA14-1. Although the Ca^{2+} increase was transient, the levels remained marginally higher in sHA14-1-treated cells compared to control cells. Most of this Ca^{2+} increase could be reduced by the addition of EGTA, a Ca^{2+}-specific chelator. In addition, classical antioxidants, such as MnTBAP, Trolox, and the mitochondrially-targeted compound MitoQ10, also attenuated the Ca^{2+} increase. Low concentrations of sHA14-1 also induced

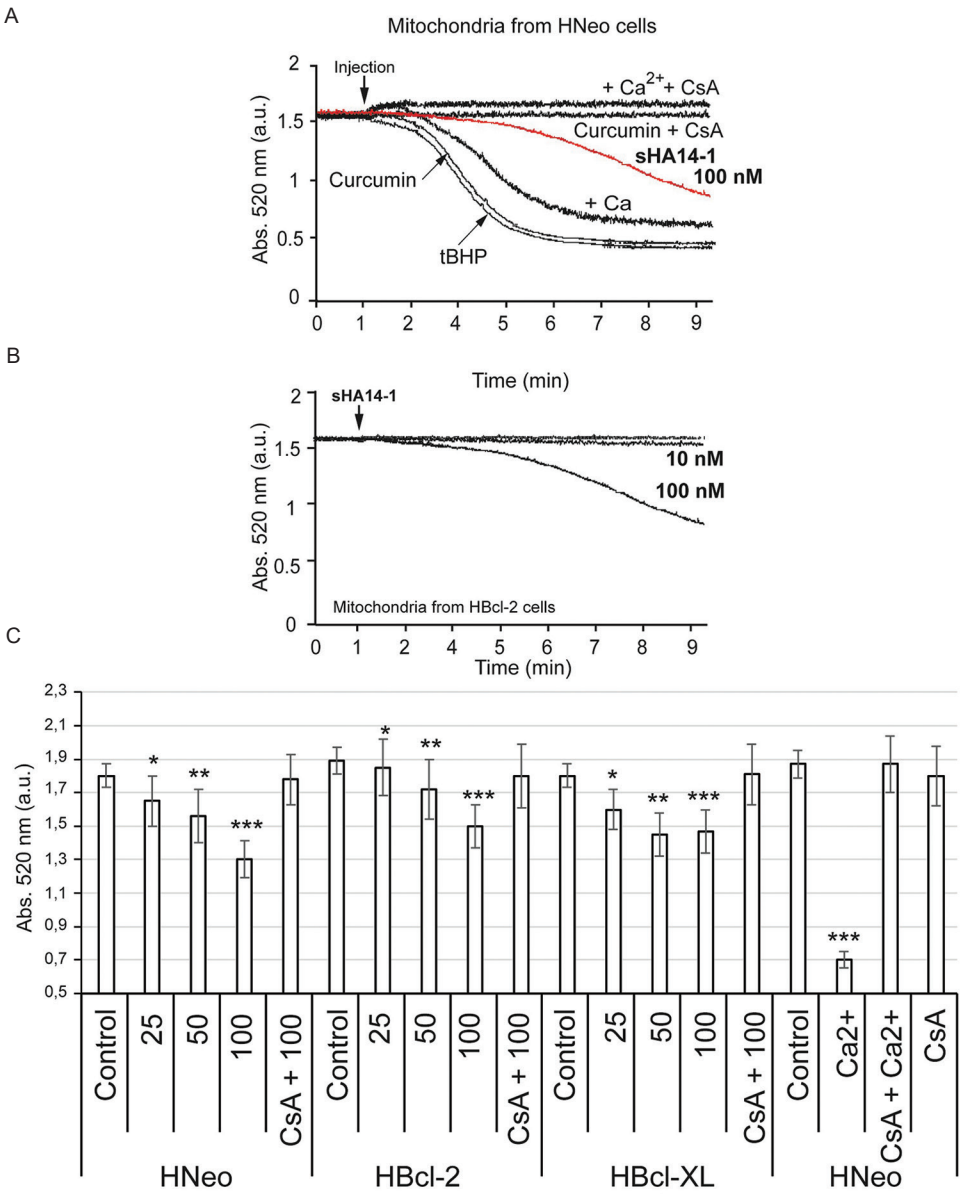

Figure 6. Permeability transition pore opening induced by sHA14-1 in isolated and purified mitochondria from Hela cells. (A) Control mitochondria from HNeo cells undergo prototypical permeability transition pore (PTP) opening in response to calcium, curcumin, or tert-butyl hydroperoxide (tBHP). HA14-1 was added at 50 nM. (B) Mitochondria from HBcl-2 cells treated with 10 and 100 nM sHA14-1. (C) Histograms of mitochondria from the three cell types (HNeo, HBcl-2, and HBcl-XL) treated with SHA14-1 at different concentrations. The prototypical opening of PTPs by calcium (1 mM) is presented for comparison.

Abbreviations: Abs: Absorbance; Bcl-XL: B-cell lymphoma-extra-large; Bcl-2: B-cell lymphoma 2; Ca^{2+}: Calcium. Notes: CsA refers to cyclosporine A at a concentration of 2 mM. HNeo represents control HeLa cells transfected with the pcDNA3.1 vector containing the neomycin-resistance gene. HBcl-2 refers to HeLa cells transfected with the human *BCL-2* gene. HBcl-XL are cells transfected with the human *BCL-XL* gene.

Note: *p<0.05, **p<0.01, ***p<0.001.

the hydrogen peroxide production (Figure 7B), which was almost completely abolished by MitoQ10. Using CMXRos, we detected a transient mitochondrial hyperpolarization, likely linked to Ca^{2+} entry into the mitochondrial matrix (Figure 7C). The increases in Ca^{2+} and ROS production followed similar patterns and paralleled the increase in mitochondrial ΔΨm (Figure 7D), with MitoQ10 effectively abolishing the transient elevation in ΔΨm (Figure 7D).

The effects of sHA14-1 on Ca^{2+} availability and on ROS production in the presence and absence of EGTA in Hneo, HBcl-2, and HBCL-XL cells are shown in Figure 7E and F. The Ca^{2+} and ROS increases in response to sHA14-1 treatment were lower in HBcl-2 and HBcl-XL cells compared to HNeo cells, and the addition of EGTA reduced the Ca^{2+} increases in both Bcl-overexpressing cell lines (Figure 7E). We also tested the effects of several antioxidants and EGTA on the sHA14-1-induced Ca^{2+} increase in HNeo cells (Figure 7F), while EGTA

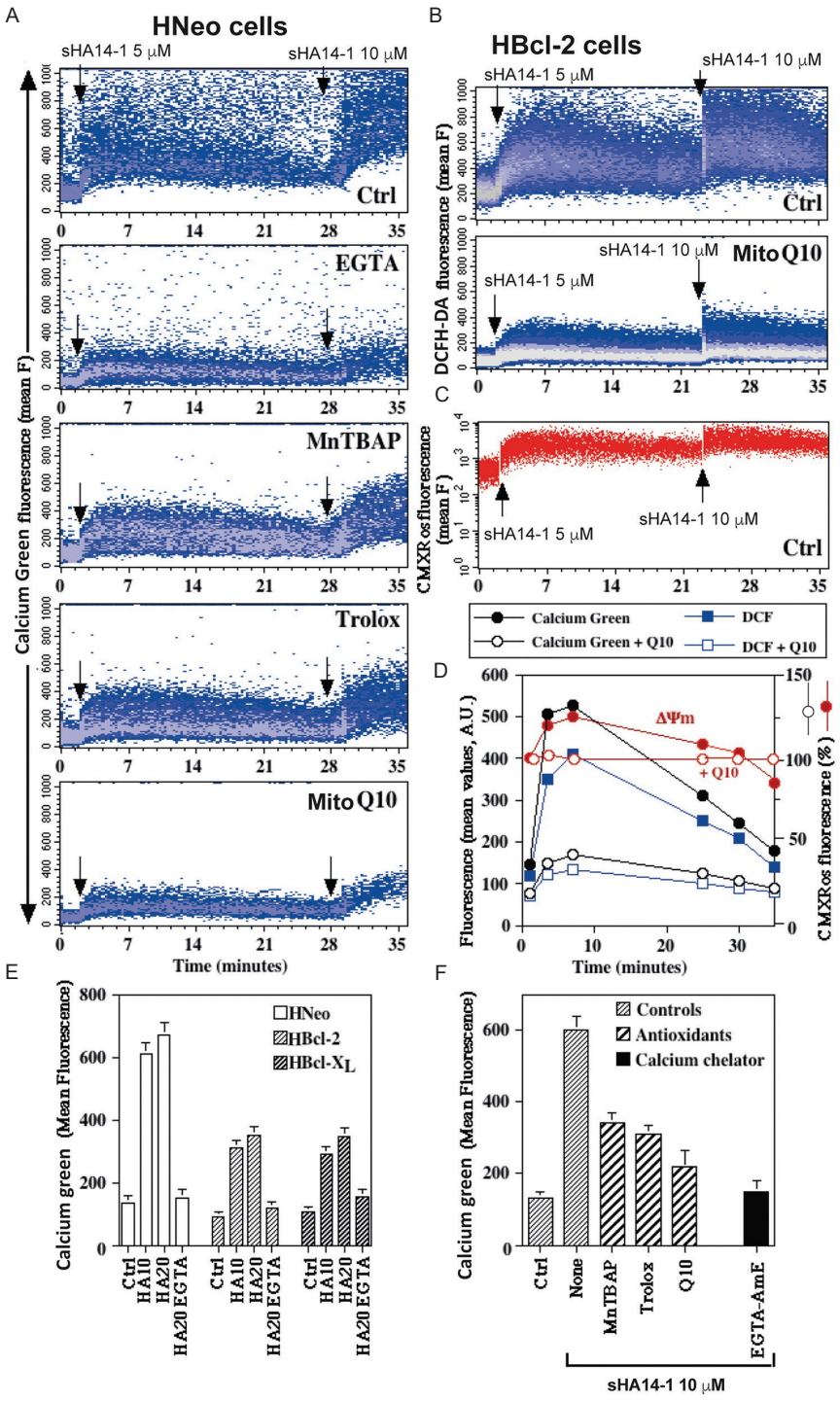

Figure 7. Flow cytometrical analysis of intracellular calcium release and reactive oxygen species production induced by sHA14-1. (A) Calcium green fluorescence was used to detect the time-dependent elevation of intracellular calcium in HNeo cells in response to sHA14-1 alone and in the presence of ethylene glycol-bis(β-aminoethyl ether)-N,N,N',N'-tetraacetic acid (EGTA; a calcium chelator) and the reactive oxygen species (ROS) inhibitors manganese (III) tetrakis (4-benzoic acid) porphyrin chloride (MnTBAP), Trolox, and mitochondrially-targeted compound (MitoQ10). (B) ROS production was measured by detecting hydrogen peroxide using dichlorofluorescein diacetate (DCFH-DA) in the presence or absence of MitoQ10. (C) Membrane potential (ΔΨm) was determined using chloromethyl-X-Rosamine (CMXRos). (D) A summarized view of the data from panels (A), (B), and (C), shown on a 35-min time scale with modulation by MitoQ10. These measurements include mitochondrial ΔΨm, measured with CMXRos, with red circles • representing ΔΨm and hollow red circle ◦ indicating ΔΨm in the presence of MitoQ10. (E) Calcium release in HNeo, HBcl-2, and HBcl-XL cells in the presence or absence of EGTA. (F) Summary of the effect of 10 μM sHA14-1 on calcium release in HNeo cells.

Abbreviations: Bcl-XL: B-cell lymphoma-extra-large; Bcl-2: B-cell lymphoma 2; Ctrl: Control; HA10: sHA14-1 at 10 μM; HA20: sHA14-1 at 20 μM; Q10: Mitochondrially-targeted compound.

Notes: HNeo represents control HeLa cells transfected with the pcDNA3.1 vector containing the neomycin-resistance gene. HBcl-2 refers to HeLa cells transfected with the human *BCL-2* gene. HBcl-XL are cells transfected with the human *BCL-XL* gene.

reduced the rise in Ca^{2+} caused by sHA14-1 as expected, antioxidants, such as Trolox and MnBTAP, also partially lowered the Ca^{2+} level. Moreover, the mitochondrially targeted antioxidant MitoQ10 almost completely abolished this sHA14-1-induced Ca^{2+} release (Figure 7F).

4. DISCUSSION

We presented an exhaustive study of the effects of sHA14-1 on three HeLa cell lines: two that overexpressed either Bcl-2 or Bcl-XL, and a control cell line with the Neo vector.

sHA14-1 is a more stable analog of HA14-1, designed to bind a functional pocket on the surface of Bcl-2 proteins, thereby blocking their activity and inducing apoptosis in cancer cells [49]. sHA14-1 has been shown to bind to all three BH1, BH2, and BH3 pockets on the Bcl-2 molecule. In contrast, sHA14-1 interacts with Bcl-XL differently, partially occupying only the BH1 and BH3 domains of its hydrophobic pocket, and potentially interacting with other vital amino acids [48]. Importantly, sHA14-1 does not bind or form complexes with Bax and/or Bak [48].

sHA14-1 reportedly has a reduced tendency to generate ROS [44] compared to HA14-1, a property that allows for more specific attribution of ROS production to mitochondria. We investigated the *in vitro* activity of sHA14-1 in inducing cell death in these HeLa cell lines, as overexpression of the Bcl-2 and Bcl-XL proteins is known to block apoptosis induced by various drugs or apoptotic inducers [56]. Our results showed that sHA14-1 effectively induced cell death in all three cell lines (HNeo, HBcl-2, and HBcl-XL) (Figure 1A and B). It is worth noting that the levels of Bcl-2 and Bcl-XL were very low in HNeo cells (Figure 1G). The ratio of apoptotic to necrotic cells varied, depending on the presence or absence of Bcl-2 or Bcl-XL. In the Bcl-2 and Bcl-XL overexpressing cells (HBcl-2 or HBcl-XL), we detected a dose-dependent induction of cell death that mimicked secondary necrosis, that is, necrosis following an apoptotic process, rather than classical apoptosis (Figure 1E and F). This tendency is often related to the kinetics of apoptosis induction, as the short duration of signal transduction pathways may prevent the full development of typical apoptotic characteristics [58]. In contrast, in HNeo cells, sHA14-1 initially induced apoptosis, which was later replaced by necrosis (Figure 1D).

Nevertheless, the cell death signal transduction we observed involved a reduction in $\Delta\Psi m$, caspase-3 activation, and exposure of phosphatidylserine residues on the outer surface of the plasma membrane (Figure 2). The addition of permeability transition blockers, such as CsA and BA, partially reduced cell death. Caspase-3 activation and inhibition experiments showed that the Bok-D inhibitor failed to fully block caspase-3 activity (Figure 3). These results sharply contrast with previous findings suggesting weak caspase activation by sHA14-1 [46], and they are inconsistent with a caspase-independent mechanism of cell death [59]. Thus, the mode of action of sHA14-1 appears to involve a mitochondrial catastrophe, coupled with classical apoptosis driven by caspase activation. However, we propose that the apoptotic phase may be brief, rapidly transitioning to a secondary necrosis-like phenotype.

In our experiments, the cellular rugosity observed in sHA14-1-treated cells, which is associated with plasma membrane permeabilization, likely reflects a rapid induction of cell death in which normal apoptotic processes cannot take place, leading to secondary necrosis (Figure 4). The altered light-scattering properties of sHA14-1-treated cells, as observed in another study [46], can be attributed to this phenomenon, in addition to the classical changes in light scattering induced by Ca^{2+} release into the cytoplasm.

Similar activities of sHA14-1 were demonstrated in isolated mitochondria. Immediately after the addition of sHA14-1, mitochondrial respiration became uncoupled, and mitochondrial $\Delta\Psi m$ dropped (Figure 4). This effect on $\Delta\Psi m$ was concentration-dependent, with the highest dose (100 μM) reducing $\Delta\Psi m$ to the level of a resting potential. This may be explained by the toxic effects of sHA14-1 on mitochondria, which require an intact ER to fully manifest. In the purified mitochondrial preparations in these experiments, only traces of ER membranes were present.

sHA14-1 also exhibited PTP-opening capabilities, though these appeared to be non-canonical. At higher concentrations, the PTPs opened only slightly, and this response differed from the typical PTP opening induced by Ca^{2+} alone. This may explain why CsA only partially rescued cells from sHA14-1-induced cell death (Figure 3).

The anti-apoptotic functions of Bcl-2 are thought to arise from its location in the mitochondrial membrane [60-62], where it regulates pro-apoptotic members of the Bcl-2 protein family [4]. Recent evidence suggested a companion role for ER-derived Bcl-2 proteins. Moreover, cross-talk between organelles, particularly between ER and mitochondria, may be more extensive than previously appreciated, especially during the induction of many apoptotic pathways [50]. For example, a recombinant form of Bcl-2, Bcl-2/cb5, which resides exclusively in the ER, has been shown to prevent apoptosis in many cell types [63,64]. However, those mediators, beyond Ca^{2+} and oxidants, that connect the ER to mitochondria remain unidentified. Clearly, intracellular Ca^{2+} signaling plays a crucial role in this process. Bcl-2 overexpression has been shown to block both Ca^{2+} entry into the ER and its release from the ER in response to apoptotic stimuli. Specifically, Bcl-2 overexpression reduces ER Ca^{2+} load [10,13,18] prevents or delays ER Ca^{2+} depletion [18] after

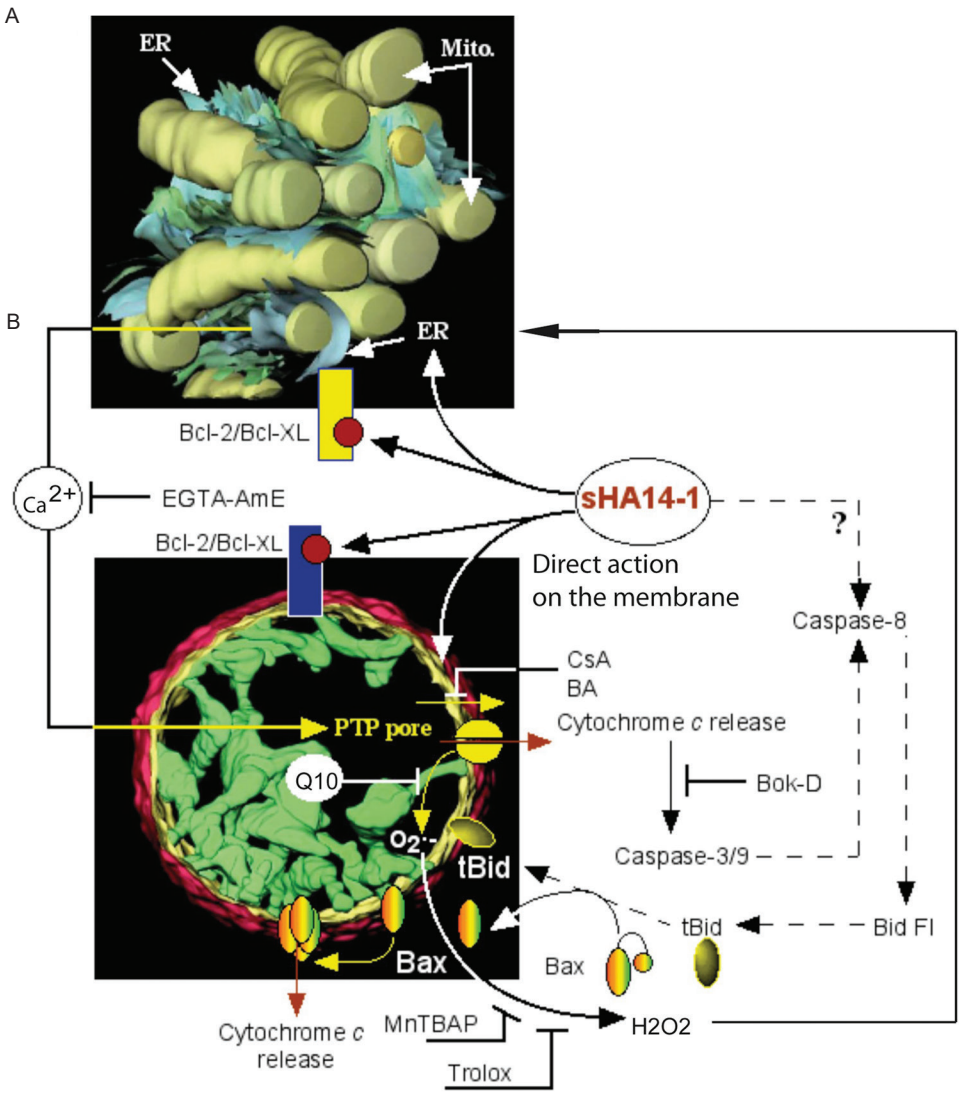

Figure 8. Schematic interpretation of sHA14-1's interactions with the endoplasmic reticulum and mitochondria. The capacity of the small molecule sHA14-1 to target multiple subcellular compartments is described. (A) A three-dimensional (3D) representation of a cluster of 14 mitochondria (mito, yellow) in the vicinity of a multilayered endoplasmic reticulum (ER, blue-green) stack. The image depicts the ER in close proximity to mitochondria, demonstrating how the ER and mitochondria may be tethered together. The close proximity of the mitochondrial and ER membranes is important for regulating cellular calcium (Ca^{2+}) levels. (B) A 3D reconstruction of a mitochondrion [82] [source: http://www.wadsworth.org], showing the mechanical effects of sHA14-1 on mitochondria. sHA14-1 targets anti-apoptotic Bcl-2 family members in both the ER and mitochondria, but it also exerts direct effects on both the ER and mitochondrial outer membranes. sHA14-1 induces Ca^{2+} release from the ER (which can be blocked by ethylene glycol-bis(β-aminoethyl ether)-N,N,N',N'-tetraacetic acid [EGTA]). It destabilizes mitochondrial bioenergetics through interactions with pro-apoptotic Bcl-2 family members, facilitating truncate Bid (tBid) action and Bcl-2 antagonist X (Bax) oligomerization, which results in permeability transition pore (PTP) opening and cytochrome c release. These events can be inhibited by PTP inhibitors such as cyclosporine A (CsA, 2 µM) and bongkrekic acid (BA, 100 nM). In addition, sHA14-1 interacts with and destabilizes the mitochondrial membrane, inducing ROS production, which can be inhibited by antioxidants such as Trolox, manganese (III) tetrakis (4-benzoic acid) porphyrin chloride (MnBTAP), and mitochondrially-targeted compound (MitoQ10). This creates a vicious cycle, enhancing mitochondrial damage and further ER Ca^{2+} release. The question mark (?) indicates a possible direct interaction between sHA14-1 and caspase-8, which remains unproven.
Abbreviations: Bcl-XL: B-cell lymphoma-extra-large; Bcl-2: B-cell lymphoma 2; Bid F1: Bid, a pro-apoptotic member of the Bcl-2 family full length); Boc-D: Caspase-3 inhibitor; O_2: Oxygen.

cells are treated with thapsigargin [65,66] and/or prevents apoptosis induced by cyclopiazonic acid, ceramide, and other apoptotic inducers [9].

Transient increases in cytosolic Ca^{2+} activate numerous cytosolic enzymes, such as phospholipases, proteases, and endonucleases. However, unregulated or prolonged increases in cytosolic Ca^{2+} [67] above a certain threshold can lead to apoptosis or cell death [8,67-69]. Several mechanisms contribute to the induction of cell death through elevated or transient Ca^{2+} spikes. These include the direct effects of

Ca^{2+} accumulation within mitochondria, which can trigger PTP opening, as well as the activation of caspase-12 and/or other intracellular Ca^{2+}-sensitive enzymes [70]. The ER and mitochondria are physiologically interconnected and crucial for the regulation of intracellular Ca^{2+} homeostasis. Under certain conditions, rapid Ca^{2+} accumulation and Ca^{2+}-mediated signaling between mitochondria occur following an initial release of Ca^{2+} from the ER [71,72]. This rapid rise in Ca^{2+} near the mitochondria may initiate a cascade of events, including a rapid influx of Ca^{2+} into the mitochondria, PTP opening, increased mitochondrial membrane permeability, mitochondrial alteration, ROS production, and, ultimately, cytochrome c release. ROS are potent inducers of cytochrome c release because they accentuate mitochondrial membrane permeability and induce phospholipid peroxidation, rendering cytochrome c more readily available for release. With regard to the mode of action of sHA14-1, it appears to affect ER-mediated Ca^{2+} release, which can be blocked by the Ca^{2+} chelator EGTA and the mitochondrially targeted antioxidant MitoQ10. These results validated earlier observations of Hermanson *et al.* [46], who implicated the ER in sHA14-1 actions. Taken together, these data suggest that a complex mechanism involving both mitochondria and ER is at work during sHA14-1 treatments.

Thus, sHA14-1, an antagonist of anti-apoptotic Bcl-2 proteins (Bcl-2/Bcl-XL), exhibits multiple additional effects (Figure 8). While sHA14-1 primarily targets Bcl-2 and Bcl-XL, it also substantially affects mitochondrial and ER membranes. As previously described, some of its effects may be mediated by a reduction in the activity of SERCAs in the ER [46]. At the ER-mitochondria junctions (MAMs), Ca^{2+} uptake occurs locally through SERCAs, which normally attenuates the mitochondrial response to continuous Ca^{2+} release through IP3R activity or during gradual Ca^{2+} influx near MAMs [71]. In addition, a direct effect on mitochondria, though, affecting mitochondrial membrane structures, bioenergetics, and PTP opening, is conspicuous. Although a direct interaction between sHA14-1 and mitochondrial cardiolipin has not been described, it remains a plausible hypothesis, particularly given that the PTP is affected.

It remains unclear whether sHA14-1 and similar small molecules can be considered viable cancer therapies, given that their lack of target specificity may lead to undesirable side effects. However, recent advances in the field have focused on more specific and less toxic compounds [73,74] that target proteins with greater precision, such as Venetoclax for Bcl-2 [75-77] and Navitoclax for Bcl-XL and Bcl-2 [78]. These newer molecules appear to be effective in the nm range without the toxic side effects, likely due to their specific targeting of mitochondrial/ER contact sites.

5. CONCLUSION

It remains to be determined whether sHA14-1 and similar small molecules can be considered as viable cancer therapies if their lack of target specificity contributes to undesirable effects. It seems that the progress in this field has been made with more specific and less toxic compounds [73,74] that are more specifically targeted, such as Venetoclax for Bcl-2 [73-75] and Navitoclax for Bcl-XL and Bcl-2 [76]. Apparently, these recent molecules are efficient in the nm range without toxic side effects due to their specific targeting to mitochondrial/ER contact sites.

ACKNOWLEDGMENTS

The authors kindly acknowledge Axel Kahn and Hélène Gilgenkrantz for granting us access to the Bcl-2- and Bcl-XL-expressing mice.

FUNDING

This work was supported by funding dedicated to fundamental research from the National Center for Scientific Research (CNRS) and the National Institute of Health and Medical Research (INSERM).

CONFLICT OF INTEREST

The authors declare no conflicts of interest.

AUTHOR CONTRIBUTIONS

Conceptualization: Patrice X. Petit
Formal analysis: Aoula Moustapha, Pauline Andreu, François Gonzalvez, Delphine Fradin, Jean-Pierre Tissier, Patrice X. Petit
Investigation: Aoula Moustapha, Pauline Andreu, François Gonzalvez, Delphine Fradin, Jean-Pierre Tissier, Patrice X. Petit
Methodology: Aoula Moustapha, Pauline Andreu, François Gonzalvez, Delphine Fradin, Jean-Pierre Tissier, Patrice X. Petit
Writing – original draft: Patrice X. Petit, Aoula Moustapha
Writing – review & editing: All authors

ETHICAL APPROVAL AND CONSENT TO PARTICIPATE

All experimental protocols complied with CNRS and INSERM regulations and were approved by the Small Animals Committee of the CNRS affiliated to the Cochin Institute. The relevant methods were carried out in accordance with relevant regulations and are reported in accordance with the "Animal Research: Reporting of *In Vivo* Experiments" guidelines. The transgenic animals were generated according

to the institutional rules in effect at the time of their creation (the Bcl-2 mice by Lacronique *et al.* [79] and the Bcl-XL mice by De La Coste *et al.* [80,81]).

CONSENT FOR PUBLICATION

Not applicable.

AVAILABILITY OF DATA

The datasets generated and/or analyzed during the present study are not publicly available, as the data remain the property of INSERM and CNRS. However, they are available from the corresponding author on reasonable request.

REFERENCES

1. Reed JC. Apoptosis-based therapies. *Nat Rev Drug Discov.* 2002;1(2):111-121. doi: 10.1038/nrd726
2. Tsujimoto Y, Shimizu S. Bcl-2 family: Life-or-death switch. *FEBS Lett.* 2000;466(1):6-10. doi: 10.1016/s0014-5793(99)01761-5
3. Adams JM, Cory S. Life-or-death decisions by the Bcl-2 protein family. *Trends Biochem Sci.* 2001;26(1):61-66. doi: 10.1016/s0968-0004(00)01740-0
4. Chipuk JE, Moldoveanu T, Llambi F, Parsons MJ, Green DR. The BCL-2 family reunion. *Mol Cell.* 2010;37(3):299-310. doi: 10.1016/j.molcel.2010.01.025
5. Tsujimoto Y, Cossman J, Jaffe E, Croce C. Involvement of the bcl-2 gene in human follicular lymphona. *Science.* 1985;228:1440-1443. doi: 10.1126/science.3874430
6. Krajewski S, Tanaka S, Takayama S, Schibler MJ, Fenton W, Reed JC. Investigation of the subcellular distribution of the Bcl-2 oncoprotein: Residence in the nuclear envelope, endoplasmic reticulum, and outer mitochondrial membranes. *Cancer Res.* 1993;53:4701-4714.
7. Rong Y, Distelhorst CW. Bcl-2 protein family members: Versatile regulators of calcium signaling in cell survival and apoptosis. *Annu Rev Physiol.* 2008;70:73-91. doi: 10.1146/annurev.physiol.70.021507.105852
8. Pinton P, Giorgi C, Siviero R, Zecchini E, Rizzuto R. Calcium and apoptosis: ER-mitochondria Ca2+ transfer in the control of apoptosis. *Oncogene.* 2008;27(50):6407-6418. doi: 10.1038/onc.2008.308
9. Breckenridge DG, Stojanovic M, Marcellus RC, Shore GC. Caspase cleavage product of BAP31 induces mitochondrial fission through endoplasmic reticulum calcium signals, enhancing cytochrome C release to the cytosol. *J Cell Biol.* 2003l;160(7):1115-1127. doi: 10.1083/jcb.200212059
10. Rong YP, Bultynck G, Aromolaran AS, *et al*. The BH4 domain of Bcl-2 inhibits ER calcium release and apoptosis by binding the regulatory and coupling domain of the IP3 receptor. *Proc Natl Acad Sci U S A.* 2009;106(34):14397-1402. doi: 10.1073/pnas.0907555106
11. Eckenrode EF, Yang J, Velmurugan GV, Foskett JK, White C. Apoptosis protection by Mcl-1 and Bcl-2 modulation of inositol 1,4,5-trisphosphate receptor-dependent Ca2+ signaling. *J Biol Chem.* 2010;285(18):13678-13684. doi: 10.1074/jbc.M109.096040
12. White C, Li C, Yang J, *et al*. The endoplasmic reticulum gateway to apoptosis by Bcl-X(L) modulation of the InsP3R. *Nat Cell Biol.* 2005;7(10):1021-1028. doi: 10.1038/ncb1302
13. Chen R, Valencia I, Zhong F, *et al*. Bcl-2 functionally interacts with inositol 1,4,5-trisphosphate receptors to regulate calcium release from the ER in response to inositol 1,4,5-trisphosphate. *J Cell Biol.* 2004;166(2):193-203. doi: 10.1083/jcb.200309146
14. Li C, Fox CJ, Master SR, Bindokas VP, Chodosh LA, Thompson CB. Bcl-X(L) affects Ca(2+) homeostasis by altering expression of inositol 1,4,5-trisphosphate receptors. *Proc Natl Acad Sci U S A.* 2002;99(15):9830-9835. doi: 10.1073/pnas.152571899
15. Li C, Wang X, Vais H, Thompson CB, Foskett JK, White C. Apoptosis regulation by Bcl-x(L) modulation of mammalian inositol 1,4,5-trisphosphate receptor channel isoform gating. *Proc Natl Acad Sci U S A.* 2007;104(30):12565-12570. doi: 10.1073/pnas.0702489104
16. Sharov VS, Dremina ES, Galeva NA, Williams TD, Schoneich C. Quantitative mapping of oxidation-sensitive cysteine residues in SERCA *in vivo* and *in vitro* by HPLC-electrospray-tandem MS: Selective protein oxidation during biological aging. *Biochem J.* 2006;394(Pt 3):605-615. doi: 10.1042/BJ20051214
17. Dremina ES, Sharov VS, Kumar K, Zaidi A, Michaelis EK, Schoneich C. Anti-apoptotic protein Bcl-2 interacts with and destabilizes the sarcoplasmic/endoplasmic reticulum Ca2+-ATPase (SERCA). *Biochem J.* 2004;383(Pt 2):361-370. doi: 10.1042/BJ20040187
18. Hanson CJ, Bootman MD, Distelhorst CW, Wojcikiewicz RJ, Roderick HL. Bcl-2 suppresses Ca2+ release through inositol 1,4,5-trisphosphate receptors and inhibits Ca2+ uptake by mitochondria without affecting ER calcium store content. *Cell Calcium.* 2008;44(3):324-338. doi: 10.1016/j.ceca.2008.01.003
19. Ahmad S, Ahmad A, Dremina ES, *et al*. Bcl-2 suppresses sarcoplasmic/endoplasmic reticulum Ca2+-ATPase expression in cystic fibrosis airways: Role in oxidant-mediated cell death. *Am J Respir Crit Care Med.* 2009;179(9):816-826. doi: 10.1164/rccm.200807-1104OC
20. Dremina ES, Sharov VS, Schoneich C. Displacement of SERCA from SR lipid caveolae-related domains by Bcl-2: A possible mechanism for SERCA inactivation. *Biochemistry.* 2006;45(1):175-184. doi: 10.1021/bi050800s
21. Rizzuto R, Pinton P, Carrington W, *et al*. Close contacts with the endoplasmic reticulum as determinants of mitochondrial Ca2+ responses. *Science.* 1998;280(5370):1763-1766. doi: 10.1126/science.280.5370.1763
22. Gouriou Y, Gonnot F, Wehbi M, Brun C, Gomez L, Bidaux G. High-sensitivity calcium biosensor on the mitochondrial surface

reveals that IP3R channels participate in the reticular Ca2+ leak towards mitochondria. *PLoS One.* 2023;18(6):e0285670. doi: 10.1371/journal.pone.0285670
23. Demaurex N, Distelhorst C. Cell biology. Apoptosis--the calcium connection. *Science.* 2003;300(5616):65-67. doi: 10.1126/science.1083628
24. Lee DI, Sumbilla C, Lee M, *et al*. Mechanisms of resistance and adaptation to thapsigargin in androgen-independent prostate cancer PC3 and DU145 cells. *Arch Biochem Biophys*. 2007;464(1):19-27. doi: 10.1016/j.abb.2007.03.040
25. Liu X, Lee K, Herbison AE. Kisspeptin excites gonadotropin-releasing hormone neurons through a phospholipase C/calcium-dependent pathway regulating multiple ion channels. *Endocrinology.* 2008;149(9):4605-4614. doi: 10.1210/en.2008-0321
26. Denmeade SR, Isaacs JT. The SERCA pump as a therapeutic target: Making a "smart bomb" for prostate cancer. *Cancer Biol Ther.* 2005;4(1):14-22. doi: 10.4161/cbt.4.1.1505
27. O'Neill JP, Velalar CN, Lee DI, *et al*. Thapsigargin resistance in human prostate cancer cells. *Cancer.* 2006;107(3):649-659. doi: 10.1002/cncr.22027
28. Bollig A, Xu L, Thakur A, Wu J, Kuo TH, Liao JD. Regulation of intracellular calcium release and PP1alpha in a mechanism for 4-hydroxytamoxifen-induced cytotoxicity. *Mol Cell Biochem.* 2007;305(1-2):45-54. doi: 10.1007/s11010-007-9526-2
29. Reed JC. Mechanisms of apoptosis avoidance in cancer. *Curr Opin Oncol.* 1999;11(1):68-75. doi: 10.1097/00001622-199901000-00014
30. Jansen B, Schlagbauer-Wadl H, Brown BD, *et al*. bcl-2 antisense therapy chemosensitizes human melanoma in SCID mice. *Nat Med.* 1998;4(2):232-234. doi: 10.1038/nm0298-232
31. Huang Z. Bcl-2 family proteins as targets for anticancer drug design. *Oncogene.* 2000;19(56):6627-6631. doi: 10.1038/sj.onc.1204087
32. Liu D, Huang Z. Synthetic peptides and non-peptidic molecules as probes of structure and function of Bcl-2 family proteins and modulators of apoptosis. *Apoptosis*. 2001;6(6):453-462. doi: 10.1023/A:1012481406064
33. Muchmore SW, Sattler M, Liang H, *et al*. X-ray and NMR structure of human Bcl-xL, and inhibitor of programmed cell death. *Nature.* 1996;381:335-341. doi: 10.1038/381335a0
34. Sattler M, Liang H, Nettesheim D, *et al*. Structure of BCl-XL-Bak peptide complex: Recognition between regulators of apoptosis. *Science.* 1997;275:983-986. doi: 10.1126/science.275.5302.983
35. Ellerby HM, Arap W, Ellerby LM, *et al*. Anti-cancer activity of targeted pro-apoptotic peptides. *Nat Med*. 1999;5(9):1032-1038. doi: 10.1038/12469
36. Wang JL, Zhang ZJ, Choksi S, *et al*. Cell permeable Bcl-2 binding peptides: A chemical approach to apoptosis induction in tumor cells. *Cancer Res*. 2000;60(6):1498-1502.
37. Degterev A, Lugovskoy A, Cardone M, *et al*. Identification of small-molecule inhibitors of interaction between the BH_3 domain and Bcl-XL. *Nat Cell Biol.* 2001;3:173-182. doi: 10.1038/35055085
38. Lugovskoy AA, Degterev AI, Fahmy AF, *et al*. A novel approach for characterizing protein ligand complexes: Molecular basis for specificity of small-molecule Bcl-2 inhibitors. *J Am Chem Soc.* 2002;124(7):1234-1240. doi: 10.1021/ja011239y
39. Tzung SP, Kim KM, Basanez G, *et al*. Antimycin A mimics a cell-death-inducing Bcl-2 homology domain 3. *Nat Cell Biol.* 2001;3(2):183-191. doi: 10.1038/35055095
40. Nakashima T, Miura M, Hara M. Tetrocarcin A inhibits mitochondrial functions of Bcl-2 and suppresses its anti-apoptotic activity. *Cancer Res*. 2000;60(5):1229-1235.
41. Anether G, Tinhofer I, Senfter M, Greil R. Tetrocarcin-A--induced ER stress mediates apoptosis in B-CLL cells via a Bcl-2--independent pathway. *Blood.* 2003;101(11):4561-4568. doi: 10.1182/blood-2002-08-2501
42. Letai A. BCL-2: Found bound and drugged! *Trends Mol Med.* 2005;11(10):442-444. doi: 10.1016/j.molmed.2005.08.007
43. Letai A. Pharmacological manipulation of Bcl-2 family members to control cell death. *J Clin Invest.* 2005;115(10):2648-2655. doi: 10.1172/JCI26250
44. Tian D, Das SG, Doshi JM, Peng J, Lin J, Xing C. sHA 14-1, a stable and ROS-free antagonist against anti-apoptotic Bcl-2 proteins, bypasses drug resistances and synergizes cancer therapies in human leukemia cell. *Cancer Lett.* 2008;259(2):198-208. doi: 10.1016/j.canlet.2007.10.012
45. Reed JC. Bcl-2-family proteins and hematologic malignancies: History and future prospects. *Blood.* 2008;111(7):3322-3330. doi: 10.1182/blood-2007-09-078162
46. Hermanson D, Addo SN, Bajer AA, *et al*. Dual mechanisms of sHA 14-1 in inducing cell death through endoplasmic reticulum and mitochondria. *Mol Pharmacol*. 2009;76(3):667-678. doi: 10.1124/mol.109.055830
47. Das SG, Doshi JM, Tian D, *et al*. Structure-activity relationship and molecular mechanisms of ethyl 2-amino-4-(2-ethoxy-2-oxoethyl)-6-phenyl-4h-chromene-3-carboxylate (sha 14-1) and its analogues. *J Med Chem.* 2009;52(19):5937-5949. doi: 10.1021/jm9005059
48. Rehman K, Tariq M, Akash MS, Gillani Z, Qazi MH. Effect of HA14-1 on apoptosis-regulating proteins in HeLa cells. *Chem Biol Drug Des.* 2014;83(3):317-323. doi: 10.1111/cbdd.12245
49. Wang JL, Liu D, Zhang ZJ, *et al*. Structure-based discovery of an organic compound that binds Bcl-2 protein and induces apoptosis of tumor cells. *Proc Natl Acad Sci U S A.* 2000;97(13):7124-7129. doi: 10.1073/pnas.97.13.7124
50. Ferri KF, Kroemer G. Organelle-specific initiation of cell death pathways. *Nat Cell Biol.* 2001;3(11):E255-E263. doi: 10.1038/ncb1101-e255
51. Hoth M, Button DC, Lewis RS. Mitochondrial control of calcium-channel gating: A mechanism for sustained signaling

and transcriptional activation in T lymphocytes. *Proc Natl Acad Sci U S A.* 2000;97(19):10607-10612. doi: 10.1073/pnas.180143997

52. Dolman NJ, Gerasimenko JV, Gerasimenko OV, Voronina SG, Petersen OH, Tepikin AV. Stable Golgi-mitochondria complexes and formation of Golgi Ca(2+) gradients in pancreatic acinar cells. *J Biol Chem.* 2005;280(16):15794-15799. doi: 10.1074/jbc.M412694200
53. Csordas G, Thomas AP, Hajnoczky G. Quasi-synaptic calcium signal transmission between endoplasmic reticulum and mitochondria. *EMBO J.* 1999;18(1):96-108. doi: 10.1093/emboj/18.1.96
54. Kamo N, Muratsugu M, Hongoh M, Kobatake Y. Membrane potential of mitochondria measured with an electrode sensitive to tetraphenyl phosphonium and relationship between proton electrochemical potential and phosphorylation potential in steady state. *J Membr Biol.* 1979;49:105-121. doi: 10.1007/BF01868720
55. Rottenberg H. Membrane potential and surface potential in mitochondria: Uptake and binding of lipophilic cations. *J Membrane Biol.* 1984;81:127-138. doi: 10.1007/BF01868977
56. Gendron MC, Schrantz N, Metivier D, *et al*. Oxidation of pyridine nucleotides during Fas- and ceramide-induced apoptosis in Jurkat cells: Correlation with changes in mitochondria, glutathione depletion, intracellular acidification and caspase 3 activation. *Biochem J.* 2001;353(Pt 2):357-367.
57. Filippin L, Magalhaes PJ, Di Benedetto G, Colella M, Pozzan T. Stable interactions between mitochondria and endoplasmic reticulum allow rapid accumulation of calcium in a subpopulation of mitochondria. *J Biol Chem.* 2003;278(40):39224-39234. doi: 10.1074/jbc.M302301200
58. Kroemer G, Petit PX, Zamzami N, Vayssière JL, Mignotte B. The biochemistry of programmed cell death. *FASEB J.* 1995;9:1277-1287. doi: 10.1096/fasebj.9.13.7557017
59. Tait SW, Green DR. Caspase-independent cell death: Leaving the set without the final cut. *Oncogene.* 2008;27(50): 6452-6461. doi: 10.1038/onc.2008.311
60. Vander Heiden MG, Chandel NS, Williamson EK, Schumacker PT, Thompson CB. Bcl-xL regulates the membrane potential and volume homeostasis of mitochondria. *Cell.* 1997;91(5):627-637. doi: 10.1016/s0092-8674(00)80450-x
61. Vander Heiden MG, Chandel NS, Schumacker PT, Thompson CB. Bcl-xL prevents cell death following growth factor withdrawal by facilitating mitochondrial ATP/ADP exchange. *Mol Cell.* 1999;3(2):159-167. doi: 10.1016/s1097-2765(00)80307-x
62. Yang J, Liu X, Bhalla K, *et al*. Prevention of apoptosis by Bcl-2: Release of cytochrome C from mitochondria blocked. *Science.* 1997;275:1129-1132. doi: 10.1126/science.275.5303.1129
63. An J, Chen Y, Huang Z. Critical upstream signals of cytochrome C release induced by a novel Bcl-2 inhibitor. *J Biol Chem.* 2004;279(18):19133-19140. doi: 10.1074/jbc.M400295200
64. Hacki J, Egger L, Monney L, Conus S, Rosse T, Fellay I, Borner C. Apoptotic crosstalk between the endoplasmic reticulum and mitochondria controlled by Bcl-2. *Oncogene.* 2000;19(19):2286-2295. doi: 10.1038/sj.onc.1203592
65. Wagner-Souza K, Echevarria-Lima J, Rodrigues LA, Reis M, Rumjanek VM. Resistance to thapsigargin-induced intracellular calcium mobilization in a multidrug resistant tumour cell line. *Mol Cell Biochem.* 2003;252(1-2):109-116. doi: 10.1023/a:1025586225941
66. Wei H, Wei W, Bredesen DE, Perry DC. Bcl-2 protects against apoptosis in neuronal cell line caused by thapsigargin-induced depletion of intracellular calcium stores. *J Neurochem.* 1998;70(6):2305-2314. doi: 10.1046/j.1471-4159
67. Rizzuto R, Pinton P, Ferrari D, *et al*. Calcium and apoptosis: Facts and hypotheses. *Oncogene.* 2003;22(53):8619-8627. doi: 10.1038/sj.onc.1207105
68. Zecchini E, Siviero R, Giorgi C, Rizzuto R, Pinton P. Mitochondrial calcium signalling: Message of life and death. *Ital J Biochem.* 2007;56(4):235-242.
69. Pinton P, Ferrari D, Rapizzi E, Di Virgilio F, Pozzan T, Rizzuto R. A role for calcium in Bcl-2 action? *Biochimie.* 2002;84(2-3):195-201. doi: 10.1016/s0300-9084(02)01373-1
70. Li L, Cao Z, Jia P, Wang Z. Calcium signals and caspase-12 participated in paraoxon-induced apoptosis in EL4 cells. *Toxicol In Vitro.* 2010;24(3):728-736. doi: 10.1016/j.tiv.2010.01.005
71. Csordas G, Hajnoczky G. Sorting of calcium signals at the junctions of endoplasmic reticulum and mitochondria. *Cell Calcium.* 2001;29(4):249-262. doi: 10.1054/ceca.2000.0191
72. Sergeev IN. Genistein induces Ca2+ -mediated, calpain/caspase-12-dependent apoptosis in breast cancer cells. *Biochem Biophys Res Commun.* 2004;321(2):462-467. doi: 10.1016/j.bbrc.2004.06.173
73. Xu J, Dong X, Huang DCS, Xu P, Zhao Q, Chen B. Current advances and future strategies for BCL-2 inhibitors: Potent weapons against cancers. *Cancers* (*Basel*). 2023;15(20):4957. doi: 10.3390/cancers15204957
74. Diepstraten ST, Anderson MA, Czabotar PE, Lessene G, Strasser A, Kelly GL. The manipulation of apoptosis for cancer therapy using BH3-mimetic drugs. *Nat Rev Cancer.* 2022;22(1):45-64. doi: 10.1038/s41568-021-00407-4
75. Anderson MA, Deng J, Seymour JF, *et al*. The BCL2 selective inhibitor venetoclax induces rapid onset apoptosis of CLL cells in patients via a TP53-independent mechanism. *Blood.* 2016;127(25):3215-3224. doi: 10.1182/blood-2016-01-688796
76. Roberts AW, Davids MS, Pagel JM, *et al*. Targeting BCL2 with venetoclax in relapsed chronic lymphocytic leukemia. *N Engl J Med.* 2016;374(4):311-322. doi: 10.1056/NEJMoa1513257

77. Roberts AW, Huang D. Targeting BCL_2 with BH3 mimetics: Basic science and clinical application of venetoclax in chronic lymphocytic leukemia and related B cell malignancies. *Clin Pharmacol Ther.* 2017;101(1):89-98. doi: 10.1002/cpt.553
78. Wilson WH, O'Connor OA, Czuczman MS, *et al*. Navitoclax, a targeted high-affinity inhibitor of BCL-2, in lymphoid malignancies: A phase 1 dose-escalation study of safety, pharmacokinetics, pharmacodynamics, and antitumour activity. *Lancet Oncol.* 2010;11(12):1149-1159. doi: 10.1016/S1470-2045(10)70261-8
79. Lacronique V, Mignon A, Fabre M, *et al*. Bcl-2 protects from lethal hepatic apoptosis induced by an anti-Fas antibody in mice. *Nature Med.* 1996;2:80-86. doi: 10.1038/nm0196-80
80. De la Coste A, Fabre M, McDonell N, *et al*. Differential protective effects of Bcl-xL and Bcl-2 on apoptotic liver injury in transgenic mice. *Am J Physiol.* 1999;277(3 Pt 1):G702-G708. doi: 10.1152/ajpgi.1999.277.3.G702
81. De la Coste A, Fabre M, McDonnel N, *et al*. Bcl-XL and Bcl-2 differentially block fas/CD95- and TNFa-induced apoptotic liver injury in transgenic mice. *Am J Physiol.* 1998;59: 5017-5022.
82. Frey TG, Mannella CA. The internal structure of mitochondria. *Trends Biochem Sci.* 2000;25(7):319-324. doi: 10.1016/s0968-0004(00)01609-1